Isotopic composition of bare soil evaporated water vapor. Part I: RUBIC IV experimental set up and results

Isabelle Braud, P. Biron, Thierry Bariac, Patrick Richard, Laurent Canale, J.P. Gaudet, M. Vauclin

Paper published in Journal of Hydrology, 369, 1-16, 2009, 10.1016/j.jhydrol.2009.01.034

Isotopic composition of bare soil evaporated water vapor

Part I: RUBIC IV experimental setup and results

I. Braud[(1)], P. Biron[(2)], T. Bariac[(2)], P. Richard[(2)], L. Canale[(2)], J.P. Gaudet [(3)], M. Vauclin [(3)]

(1) Cemagref, UR HHLY, 3bis Quai Chauveau, 69336 Lyon Cedex 9, France

(2) BioEMCo (UMR 7618 CNRS, ENS-Ulm, ENSCP, INRA, AgroParisTech, UPMC) INRA-AgroParisTech, Bâtiment EGER, 78850 Thiverval-Grignon, France

(3) LTHE (UMR 5564 CNRS, INPG, IRD, UJF), BP 53X, 38041 Grenoble, Cédex 9, France

Corresponding author: Isabelle Braud, Cemagref, UR HHLY, 3bis Quai Chauveau, 69336 Lyon Cedex 9, France, Tel: +33 4 72 20 87 78, isabelle.braud@cemagref.fr

Summary

Stable water isotopes such as oxygen 18, are natural tracers of water movement within the soil–vegetation–atmosphere continuum. They provide useful information for a better understanding of evaporation and water vapor transport within soils. This paper presents a novel controlled experimental set up. It is dedicated to detailed measurements of the evaporation fluxes from bare soil columns, as well as to the corresponding isotopic composition of the water vapor, under non steady state conditions. The experiment allowed an accurate determination of these quantities. The formulae encountered in the literature were used to estimate the isotopic composition of the evaporated water vapor. None of them was able to correctly reproduce the measured isotopic composition of water. The data were then used to estimate the value of the isotopic composition of the soil liquid water, which should be used to get the right results for the isotopic composition of the evaporated water vapor. Results suggest that, when liquid transfer is dominant within the soil, the isotopic composition of evaporation was controlled by the isotopic composition of the liquid water within very thin soil surface layers. When there is a peak in the isotopic profile, i.e. when water vapor is dominant close to the surface, the isotopic composition of the evaporated water seems to be governed by the isotopic composition of the soil liquid water at the peak.

The data were also used to estimate the kinetic fractionation factor. The results suggest that the latter is not constant in time. The values seem to depend on the shape of the isotopic profile. In both cases, the uncertainty on the results is very large. The estimation of the kinetic fractionation factor is studied more in details using the modeling results presented in Part II of a companion paper where the data set is modeled using the SiSPAT_Isotope model.

Keywords: Soil water, Water vapor, Soil evaporation, Oxygen 18, Kinetic fractionation factor, RUBIC IV reactor, Laboratory experiment

1. Introduction

Evaporation from soils and transpiration by vegetation represent the major rainfall-recycling source over continents (Chahine, 1992, Parlange and Katul, 1992; Costanza et al., 1997; Zangvil et al., 2004). Consequently, a correct assessment of potential impacts of water management practices, land use and/or climate change on water resources relies on an accurate representation of evapotranspiration within atmosphere, hydrological or vegetation models. Soil Vegetation Atmosphere Transfer (SVAT) models represent the complex interactions between the atmosphere, the soil and the biosphere. Most of them provide separate estimates of soil evaporation, interception by the canopy and transpiration by plants. However, few data (relying mainly on sap flow and micro-lysimeters measurements) are currently available to validate that partition. Stable water isotopes are natural tracers of water movement. They can provide useful information to quantify and understand this partition (Yakir and Sternberg, 2000; Yepez et al., 2003; Williams et al., 2004). The isotopic composition of water within soils is known to be modified under soil evaporation (i.e. Barnes and Allison, 1983), whereas no fractionation of isotopic forms of either oxygen or hydrogen occurs during root extraction (Zimmermann et al., 1967; Walker and Richardson, 1991; Bariac et al., 1994). The isotopic composition of evaporated and transpired water vapor is therefore expected to be different. In the field however, they cannot be measured separately as they are instantaneously mixed with the ambient air water vapor. It is therefore necessary to estimate them from measurements of the isotopic composition of liquid water in soils, leaves and stems (e.g. Yakir and Sternberg, 2000; Yepez et al., 2003; Williams et al., 2004) with formulae established for water bodies or oceans such as the Craig and Gordon (1965) model (Yakir and Sternberg, 2000). Their use for deriving the isotopic composition of soil evaporated water vapor is particularly critical, as soils are generally unsaturated and the

evaporation front moves below the surface as the soil dries out. To study the mechanisms controlling the isotopic composition of evaporating soils, we have developed a physically based model, called SiSPAT_Isotope (Braud et al., 2005a) for bare soil, representing the full interactions between the atmosphere, the soil and stable isotope species. The model was evaluated against two sets of laboratory data (Braud et al., 2005b). The data were composed of soil columns which were let evaporating freely in the atmosphere. The results of this first study showed that lots of uncertainty in the modeling and interpretation of stable isotope composition of water in terms of evaporation were related to a lack of control of the experimental conditions, especially of the atmospheric relative humidity and to a lack of knowledge of the kinetic fractionation factor for unsaturated soils. In this paper, we present a novel controlled experiment dedicated to the measurement of the evaporation flux from bare soil columns, as well as its isotopic composition. The experimental set up allowed a precise determination of the atmospheric conditions, of the evaporation fluxes and of their isotopic composition. In addition, the data provide an evaluation of the formulae traditionally used for deriving the isotopic composition of bare soil evaporated water vapor, and especially of the relevance of the kinetic fractionation factor values proposed in the literature for free water bodies (Merlivat and Jouzel, 1979; Cappa et al., 2003). We also propose estimations of this kinetic fractionation factor and of its associated standard error with the experimental data. Data interpretation was found to be very sensitive to the value of the isotopic composition of the soil surface liquid water. It raises questions about the relevant sampling depth which is required to properly estimate the isotopic composition of evaporated water vapor. This point is studied more in details in Part II of a companion paper (Braud et al., 2009) which presents the modeling of these experimental results using the SiSPAT_Isotope model.

2. Material and methods

2.1 Experimental set up

The RUBIC IV reactor (Figures 1 and 2) was developed in order to determine the isotopic composition of the water vapor released by an evaporating soil and to monitor its time evolution as long as the soil was drying. The leak tight experimental set up allowed to inject directly a gas flow of dry air simultaneously over six evaporating soil columns and to continuously capture all the water vapor released by evaporation by cryoscopic trapping. Therefore, the only water vapor source was that of the evaporating soil columns, without any contamination from external sources in the laboratory. Furthermore, the cryoscopic trapping ensured that all the water vapor coming from the soil evaporation was completely trapped. In the design of the experimental set up, the following constraints were taken into account:

- A continuous non destructive sampling for the water vapor phase and a destructive sampling for the liquid phase within the soil columns. That implied to dismantle the soil columns at successive dates, cut them into slices and analyze the isotopic composition of all samples, as well as their gravimetric water content
- A leak tight experimental set up with regards to external contaminations and loss of vapor or water from the system through a leak
- The continuous measurement and the regulation of climatic variables
- The continuous measurement of the most important variables describing the moisture status of the soil (water pressure and water content)

The various components of the experimental set up are detailed below.

- Air circulation and cryoscopic trapping of the water vapor (Figure 2)

In order to ensure the tightness constraints, the reactor was built in Pyrex material. It was composed of six columns, 12 cm in diameter and 50 cm in height. An argon leak test was performed in order to verify that there were no leaks. A dry air flow was continuously flowing

over the columns. The air flow, available in the laboratory was desiccated using two devices in series:

- A pressured desiccating filter (DAS1 at 0.01 µm, Domnick Hunter), delivering a dew point equivalent to -40°C (Fig. 2 (a))
- A double cryoscopic trapping (Fig. 2 (b)) in an ethanol bath at –80°C (Thermo-Neslab CC100, Cryocool 1 free immersion cooler)

The dry air was then introduced into an expansion fence (Fig. 2 (c)) where the pressure was put in equilibrium with the six columns (Fig. 2 (d)). The corresponding air pressure, temperature and humidity (in order to verify that the air was dry as expected) were first measured at this stage (Fig. 2 (e)). The dry air was then delivered individually to each soil column. The output air, once modified by the evaporation from the soil, was directed towards capacitive sensors measuring the partial pressure of the water vapor (leading to the temperature and relative humidity of the air) (Fig. 2 (f)). The choice to measure the air temperature and humidity above the columns at the outlet was dictated by the following: preliminary measurements of the air relative humidity above the soil columns highlighted some heterogeneity in the atmosphere. Therefore, it was difficult to have an identical position of the sensors above each of the six columns, due to the size of the sensors. All the heterogeneities were integrated by the measurement of the air temperature and relative humidity at the outlet. The air was then directed to mass flow controllers (Fig. 2 (g)) which regulated the vapor flux as function of a set point of the air humidity at the outlet of the columns. For this purpose a Proportional Integral Derivative-type system, which allowed accurate regulation of the relative humidity above the soil columns was used. Finally, two Cryocools (Thermo-Neslab CC100) were cooling continuously a cryoscopic device (Fig. 2 (h)), allowing to trap the whole output water vapor. At the outlet of the cryocools, a

capacitive sensor (Fig. 2 (i)) was controlling the residual water vapor content and consequently the quality of the trapping.

- Continuously measured variables

A Campbell CR23X data logger and multiplexer AM 16/32 were used to record 44 variables with a 15- min averaging time step. These variables were aimed at documenting the water mass balance of the six columns and the soil moisture status of one of them, namely column 1. The measured variables were:

- The air temperature and relative humidity at the outlet of the six columns (Vaisala HMP 45, with an accuracy of ± 0.2 °C and ± 1% of relative humidity) (12 variables). The regulation of the relative humidity of the atmosphere above the soil columns is the result of a compromise between the evaporation flux and the flux of dry air flowing through the head space of the columns. The value of the latter flux should not exceed 2.0 l min^{-1} because of the isotopic risk of fractionation of the water vapor related to the incomplete trapping of this vapor (Schoch-Fisher et al., 1983). This constraint did not enable, initially, to reach a value lower than 80% for the relative humidity regulation. Then, as the evaporation flux decreased because of the fall in the soil water content, it was necessary to decrease the value retained for the regulation of the relative humidity. The values are provided in Table 1 and Figure 3.

- The air flow: six mass flow meters (Bronkhorst EL-Flow) were under control of the previous hygrometers in order to regulate air humidity above the soil columns with an accuracy of 0.0081 l min^{-1} (6 variables)

- The column mass: column 1, where soil moisture status was monitored, was weighted using a 30 kg Sartorius balance (model CP34001, accuracy 0.2 g). The five other columns were weighted by strain gauges (Tedea 1040 load cell, range 30 kg, accuracy 4 g) which were calibrated by comparison with the Sartorius balance (6 variables). The data were filtered to smooth the values

- The temperature of the cryoscopic trapping down and upstream of the columns was measured by thermocouples of K -type (2 variables)
- The air temperature and residual air humidity were measured at the outlet of the cold traps using capacitive sensors (Vaisala HMP45) (4 variables)
- The temperature of the room was measured using a Campbell T107 thermistance (1 variable)
- The atmospheric pressure was monitored using a Vaisala PT101B barometer. The absolute pressure in the expansion fence (slightly put in over-pressure) was measured using an Edwards EPS10 gauge (2 variables)
-The soil water pressure was measured in column 1 by using ceramic porous cups (SDEC 220) of 2 mm in diameter and 20 mm in length, provided with nylon capillary tubes and connected to pressure transducers. The calibration of the pressure transducers was carried out by using the variation of a water column for the pressure below 100 hPa and a SDEC manometer between 100 and 600 hPa. The data were corrected from the air pressure variations in the reactor. Three such porous cups were installed at –2.5, -8 and -16 cm depths (3 variables)
- Capacitive moisture probes (SDEC HMS 9000) positioned at –2.5, -8, -16 and –24 cm depths were recording continuously the temperature and electric permittivity of the soil of column 1. Conversion of the permittivity values into volumetric water content ones ($(\theta_{-2.5}$; θ_{-8} ; θ_{-16} ; θ_{-24}) was performed using a calibration based on gravimetric sampling. The temperature sensors were calibrated against a K-type thermocouple using a stat-controlled water bath (8 variables). In addition, some gravimetric samples were collected for the 0-2.5 and 2.5-5 cm soil layers at various dates to determine the evolution of the surface moisture content and the isotopic composition of the liquid phase. The holes were then filled with

wood dowels and the corresponding surface was removed from the evaporating surface of the columns (note that this sampling required a temporary stop of the experiment).

- Filling of the soil columns

The soil used to fill the columns was a silt loam (18% clay, 65% loam, 17% sand). It had been collected at the field station of Lusignan (41.44°N, 0.14°W), France. The water tightness constraints did not allow the use of undisturbed soil columns. Therefore, the soil was oven-dried and sieved at 2 mm to remove stones and coarse organic matter. In order to get a dry bulk density closed to the *in situ* one (ρ_d = 1.4 g cm^{-3}), the soil was humidified using demineralized water of known isotopic composition at a constant water content corresponding to a gravimetric value of 0.14 g g^{-1}. The columns were filled with wet soil by packing successive thin layers of constant mass in order to obtain the same dry bulk density values over each column height (35 cm of soil). The columns were closed at their base by clay marbles and by filters to facilitate their water saturation. This was achieved by capillary rise from the bottom of the columns up to the soil surface using connected tanks. At the end of the saturation process, a water sample was taken at the surface and the bottom of each column to determine the isotopic composition of the water by mass spectrometry. Results given in Table 2 show a satisfying reproductibility of the initial conditions prevailing within all the columns.

- Isotopic measurements

The water samples were analyzed using mass spectrometers (OPTIMA, GV Instrument) to determine their content in oxygen 18.

During the first three months, the water vapor was trapped twice a day and then once a day as evaporation decreased. To determine the atmospheric water vapor isotope concentration, the vapor was frozen out of a maximum air flow of 1.0 l min^{-1} into a trap cooled at -80°C.

The trapped vapor was analyzed using the CO2 equilibration technique to determine the oxygen 18 composition of water. Estimated standard deviation for the samples of water vapor was $0.1^{o}/_{oo}$.

For the liquid phase of the soil samples, the water was distilled at 90°C under vacuum conditions from the material into a trap cooled by liquid nitrogen. During the static vacuum distillation used for extracting soil water, the recovery was higher than 98 %. Water content was obtained from weight loss of soil during distillation. Isotopic contents of soil water were corrected according to the distillation yield by a Rayleigh-type law (Araguas-Araguas et al., 1995). Although all the extraction carried out during the experiment had an efficiency higher than 98%, a correction, ranging from 0 to 0.4 $^{\circ}/_{\infty}$ was still necessary. The vacuum distillation technique provides accurate results, especially for soils with the highest water content. As shown in Fig. 4, no significant differences were observed during the prior tests between the isotopic composition of soil water, exfiltrated water and supply water. Indeed, the extraction temperature has been kept at a low value (90°C) in order to minimize the impact of the immobile water distillation on the isotopic composition of the extracted soil water (Araguas-Araguas et al., 1995).

Note that throughout the paper, isotope measurements will be expressed in "δ" notation, as the deviation of the isotopic ratio in parts per thousand from that of the Vienna Standard Mean Ocean Water (V-SMOW, Gonfiantini, 1978).

The experiment was launched on April 11 2005 at 12h 00 (Day of the Year: DoY 101) and lasted 338 days. At successive dates during the drying process (Table 3), one of the columns was dismantled. Soil slices were sampled throughout the profile and analyzed as described above. The thickness of the samples was about 0.5 cm between the surface and 10 cm depth and 1 cm below.

The nomenclature and list of symbols used in the following of the paper are provided in Appendix A.

2.2 Calculation of the evaporation flux and correction of the reactor dynamics

The evaporation flux was calculated using three methods (four for column 1) in order to verify mass conservation:

- Method 1. The evaporation flux was calculated using the air temperature T_{out}, relative humidity h_{uout} (-) and the mass flow q_{out} (l min^{-1}) at the outlet of the columns as:

$$E = \rho_a \frac{e_{aout} q_{out}}{\left(P_{\exp} - e_{aout}\right) S_{col}} \quad (1)$$

where E (kg m^{-2} s^{-1}) is the water vapor flux; q_{out} (m^3 s^{-1}) is the flow of water vapor; $e_{aout}=f(T_{out}, h_{uout})$ (Pa) is the water vapor pressure at the outlet of the column; P_{exp} (Pa) is the pressure in the expansion fence; ρ_a (kg m^{-3}) is the water vapor volumetric mass and S_{col} (m^2) is the evaporative surface of the column.

- Method 2. The method uses directly the continuous weighting of the columns. The evaporation flux was obtained from mass difference between two time steps, with a filtering of the results.

- Method 3. It was based on the weighting of the frozen vapor which was trapped at the outlet of the soil columns. The flux was obtained as the mass divided by the time step. Note that the time resolution of this method is coarser than methods 1 and 2, as water vapor was trapped twice or once a day.

- Method 4. For column 1, an additional method was used to check the cumulative evaporation. It was based on the calculation of the change in soil water storage ΔS between a time step and the initial value. The soil water storage variation, ΔS (m), was deduced as the integral of the soil water content using the following approximation:

$$\Delta S = 0.35\theta_s - \int_{z=0}^{z=-0.35} \theta(z)dz \approx 0.35\theta_s - \frac{0.0525\theta_{-2.5} + 0.0675\theta_{-8} + 0.08\theta_{-16} + 0.15\theta_{-24}}{0.35} \quad (2)$$

where θ_s (m^3 m^{-3})is the volumetric water content at saturation, and θ_{-i} is the volumetric water content at depth $_{-i}$, the origin (z= 0) being positively oriented downwards.

Appendix B provides the reactor equations. This Appendix shows that the approximation of equality between the water flow at the outlet and the evaporation flux was valid throughout the whole experiment. Appendix B also shows that the isotopic composition of the water vapor measured at the outlet of the columns can be assumed equal to that of the evaporated water vapor (Zimmerman et al., 1967).

2.3 Isotopic composition of evaporated water vapor

For a free water, Craig and Gordon (1965) proposed the following equation for the derivation of the isotopic composition, δ_{iE}^v , of the evaporated water vapor:

$$\delta_{iE}^v = \frac{\left(\delta_{is}^l + 1\right) - h_a^{'}\left(\delta_{ia}^v + 1\right)\left(\varepsilon_e + 1\right)}{\left(\varepsilon_e + 1\right)\left(\varepsilon_K + 1\right)\left(1 - h_a^{'}\right)} - 1 \quad (3)$$

where δ_{is}^l (resp. δ_{ia}^v) is the isotopic composition of the liquid water (resp. the ambient air water vapor), $\varepsilon_e=(1-\alpha_e)$ and $\varepsilon_K=(1-\alpha_K)$. The equilibrium isotopic fractionation factor $\alpha_e = \frac{R_i^l}{R_i^v} = \frac{1}{\alpha_e^*}$ (-) is defined as the ratio of the isotopic ratio in the liquid phase R_i^l to the isotopic ratio in the vapor phase R_i^v . Its expression is given by Majoube (1971) as a function of temperature T (K). α_K (-) is the so-called isotopic kinetic fractionation factor. It is related to the difference in diffusivity between light and heavy water molecules (Merlivat, 1978). Finally $h_a^{'}$ is the air relative humidity, normalized to the temperature of the water surface, given by:

$$h_a^{'} = h_a \frac{\rho_{sat}^v\left(T_a\right)}{\rho_{sat}^v\left(T_s\right)} \quad (4)$$

where T_a (resp. T_s) is the air (resp. surface) temperature, h_a (-) is the air relative humidity and $\rho_{sat}^{v}(T)$ is the saturated volumetric mass of the water vapor (kg m^{-3}). Therefore, Eq. (3) can be rewritten in terms of isotopic ratio, equilibrium and kinetic fractionation factor:

$$R_{iE}^{v} = \frac{1}{\alpha_K}\frac{\left(\alpha_e^{*} R_{is}^{l} - R_{ia}^{v} h_a^{'}\right)}{\left(1 - h_a^{'}\right)} \tag{5}$$

This formula, established for free water, was shown to be valid for saturated soils by Zimmerman et al. (1967) and is also widely used to derive the isotopic composition of transpired water vapor (i.e. Yakir and Strenberg, 2000). For an unsaturated soil, the extension of the Craig and Gordon (1965) approach leads to the following expression for the isotopic composition of the evaporated water vapor:

$$R_{iE}^{v} = \frac{1}{\alpha_K}\frac{\left(\alpha_e^{*} R_{is}^{l} h_s - R_{ia}^{v} h_a^{'}\right)}{\left(h_s - h_a^{'}\right)} \tag{6}$$

where h_s is the soil surface relative humidity (-). Braud et al. (2005a) provided the following expressions for the evaporation flux E (kg m^{-2} s^{-1}) and the corresponding isotopic flux E_i (kg m^{-2} s^{-1}):

$$E = \frac{\rho_a}{r_a}\left(q_s - q_a\right) \tag{7}$$

$$E_i = \frac{\rho_a}{\alpha_K r_a}\frac{M_i}{M_w}\left(R_{is}^{v} q_s - R_{ia}^{v} q_a\right) \tag{8}$$

where ρ_a (kg m^{-3}) is the air volumetric mass; q_s and q_a (kg kg^{-1}) are the specific humidity at the soil surface and in the atmosphere, respectively; r_a (s m^{-1}) is the aerodynamic resistance to heat and water vapor transfer; M_i and M_w (kg) are the molar mass of the isotopic species and of ordinary water, respectively; R_{is}^{v} and R_{ia}^{v} are the isotopic ratio of the water vapor at the surface and in the atmosphere, respectively. Braud et al. (2005a) assumed that the liquid isotopic composition R_{is}^{l} at the soil surface was in equilibrium with the water vapor, leading to:

$$R_i^v = \alpha_e^* R_i^l \quad (9)$$

The surface isotopic flux was thus rewritten as:

$$E_i = \frac{\rho_a}{\alpha_K r_a} \frac{M_i}{M_w} \left(\alpha_e^* R_{is}^l q_s - R_{ia}^v q_a \right) \quad (10)$$

The ratio of the isotope and water vapor flux is related to the isotopic ratio R_{iE}^v of the evaporating water vapor through:

$$\frac{E_i}{E} = \frac{M_i}{M_w} R_{iE}^v \quad (11)$$

Combining Eqs (7), (8) and (11), leads to the following equation:

$$\frac{E_i}{E} = \frac{1}{\alpha_K} \frac{M_i}{M_w} \frac{\left(\alpha_e^* R_{is}^l q_s - R_{ia}^v q_a \right)}{\left(q_s - q_a \right)} = \frac{M_i}{M_w} R_{iE}^v \quad (12)$$

from which the isotopic ratio of the evaporating water vapor can be deduced:

$$R_{iE}^v = \frac{1}{\alpha_K} \frac{\left(\alpha_e^* R_{is}^l q_s - R_{ia}^v q_a \right)}{\left(q_s - q_a \right)} \quad (13)$$

The difference between (13) and (6) is due to the fact that we expressed the gradient in water vapor density between the surface and the ambient air using the specific humidity instead of the relative humidity: $\rho_s^v - \rho_a^v = \rho_{air} \left(q_s - q_a \right)$, but both expressions are strictly equivalent. In the following, Eq. (6) will be used as it is more commonly encountered in the isotopic literature.

The experiment provided the data required to use Eq. (6). As a matter of fact, the soil surface temperature was measured at –2.5 cm. The gravimetric measurements of the 0-2.5 cm layer were converted into volumetric water content from the measured values of dry bulk density (Table 2). The volumetric water content was converted into water pressure *h* using the soil retention curve fitted to the Van Genuchten (1980) expression. The points were based on measured values of soil water content and soil water pressure at –2.5 cm soil depth (Fig. 5).

From the soil water pressure h, the soil surface relative humidity h_s was deduced from the Kelvin law:

$$h_s = \exp\left(-\frac{gh}{RT_s}\right) \quad (14)$$

In Eq. (14), g ($m^2\ s^{-1}$) is the acceleration of gravity and R = 461.5 J kg^{-1} is the perfect gas constant for vapor and T_s (K) is the soil surface temperature. The air temperature and humidity of the air above the soil column were assumed to be equal to those measured at the outlet of the column. As mentioned in section 2.1, the outlet measurements were integrating all the heterogeneities in the climatic variables above the soil column and thus, could be considered as representative of the values above the soil columns. The last quantity to estimate was the isotopic ratio of the soil surface liquid phase. This was achieved by the use of the isotopic composition of the gravimetric samples mentioned above. All the data are provided in Table 4. Finally, a value of the kinetic fractionation factor had to be prescribed. Various values from the literature were tested. For molecular diffusion conditions, Merlivat (1978) proposed 1.0285 for oxygen 18, whereas Cappa et al. (2003) suggested 1.03188. Under laminar situations, the kinetic fractionation factor is assumed to be $(\alpha_K)^{2/3}$ and $(\alpha_K)^{1/2}$ for turbulent conditions (Dongmann et al., 1974), leading respectively to 1.0189 and 1.014, for oxygen 18 with the Merlivat (1978) values. The values calculated using Eq. (6) were compared with the measured ones for various estimates of the kinetic fractionation factor (see the results section). The standard error in the estimation of R_{iE}^{v} is also provided. The details of its calculation are given in Appendix C, using an extension of the approach proposed by Phillips and Gregg (2001).

There was no agreement between Eq. (6) and the measured value of the isotopic composition of the evaporated water vapor. Therefore, the value of the isotopic composition of the soil

surface liquid water, R_{is}^{l} which would be required so that both values match was also calculated as

$$R_{is}^{l} = \frac{R_{iout}^{v}\left(h_s\alpha_K - h_a^{'}\left(\alpha_K - 1\right)\right)}{\alpha_e^{*}h_s} \quad (15)$$

where R_{iout}^{v} is the isotopic composition of the water vapor at the outlet of the columns. Appendix D provides the corresponding error calculation.

Note that Eq. (15) is similar to the one proposed by Barnes and Allison (1983) for the calculation of the peak value in the soil water isotopic composition profile. The major difference is that, contrarily to Barnes and Allison (1983) conditions, the soil is not under permanent regime in the condition of our experiment. Thus the isotopic composition of the evaporated water vapor is not equal to that of the capillary rises/alimentation water and was measured.

2.4 *Estimation of the kinetic fractionation factor*

Appendix B shows that, for our experimental conditions, the isotopic composition of the evaporating water vapor R_{iE}^{v} and the water vapor above the soil column R_{ia}^{v} as well as at the outlet R_{iout}^{v} were the same. Therefore, the kinetic fractionation factor can also be deduced from Eq. (15) as:

$$\alpha_K = \frac{\left(\alpha_e^{*}R_{is}^{l}h_s - R_{iout}^{v}h_a^{'}\right)}{\left(h_s - h_a^{'}\right)R_{iout}^{v}} \quad (16)$$

The data of the experiment as described in section 2.3 were used to perform these calculations. The standard error in the estimation of α_K is also given. The details of its calculation are provided in Appendix E.

3. Results and discussion

3.1 Evaporation flux

Figure 6 shows two examples (for columns 1 and 4) of the comparison between the cumulative and instantaneous evaporation flux using the four (three) methods described in section 2.2. Table 5 provides the values of the cumulative evaporation for the six columns and all the methods. It shows that, apart from the ΔS method, the agreement between the methods is very satisfying. Differences on cumulative evaporation are less than 5 mm between the methods. Figure 6 also shows that the dynamics of the fluxes is similar between the methods. Figure 7 presents the measured evaporation fluxes and the corresponding cumulative evaporation, calculated by method 1, for the six columns. Although, the filling of the soil columns was carefully conducted, a certain degree of variability between them can be observed. This means *a posteriori* that the flux measurement of each of the six columns was necessary for the modeling and correct data interpretation. Several phases in the evaporation can be distinguished. In a first phase (between DoY 101 and 130), the evaporation flux is almost constant (fluctuations are linked with the diurnal variations of the air temperature (see Figure 3 for the example of column 1), which was not regulated within the room). In a second phase, the flux decreases regularly up to DoY 207 as long as the soil surface is drying (volumetric water content at –2.5 cm, not shown). On DoY 207, the set point of air humidity was decreased from 80% to 60% in order to maintain the air flow above the columns (and to avoid a contamination of cold traps by a back flow of water vapor coming from the laboratory). This provokes a drastic increase of the evaporation flux and then another continuous decrease. The other changes in the prescribed relative humidity do not produce such peaks.

3.2 Volumetric and isotopic soil profiles

Table 2 shows that the saturation of the soil columns was in general correctly achieved with an isotopic composition of the liquid water which was equal, within ± 0.2 $^{o}/_{oo}$, at the surface and at the bottom of the column. In general, the latter were also equal, within ± 0.2 $^{o}/_{oo}$, to the isotopic composition of the saturation water which was -6.4 $^{o}/_{oo}$. It was not the case for columns 4 and 5 for which the isotopic composition of the liquid water at the bottom were 0.5 to 0.9 $^{o}/_{oo}$ higher than that of the saturation water This difference is not obvious to explain: it may be caused by leaks at the base of the soil column, isotopic variation in the source water, mixing with residual water... This difference does not affect data interpretation because we used the measured values for all the calculations and simulations. Figure 8 provides the water content and oxygen 18 isotopic ratio profiles of the six columns at dates they were dismantled. It shows the progressive drying of the soil column until the soil surface reaches an almost zero residual water content. The whole soil column is affected by the drying, and all depths are participating to evaporation. The isotopic ratio profiles show a progressive isotopic enrichment located close to the surface at the beginning of the drying process. After 163 days of drying (DoD), a back diffusion is observed with a peak at –2.5 cm. The depth of the peak increases up to –4 cm after 235 DoD and reached –10 cm after 338 DoD of drying. As proposed by Barnes and Allison (1983) and verified by Braud et al. (2005a) using the SiSPAT_Isotope model, the depth of the isotopic ratio peak can be associated with the depth of the evaporation front, i.e. the depth above which water vapor transport is dominant as compared to the liquid one.

3.3 Isotopic composition of the evaporated water vapor

The oxygen 18 isotopic composition of the water vapor at the outlet of the columns is shown in Fig. 9. As observed for the evaporation flux, there is certain variability amongst the six columns. This confirms the importance of having measured the flux and isotopic composition

of the evaporated water vapor of each soil column separately. The shape of the various curves is comparable. A rapid increase of the isotopic composition of the evaporated water vapor is first observed. Then a stabilization around an almost constant value can be noticed. The latter is close to the value of the initial water (-6.4 $^{o}/_{oo}$). Then, the isotopic composition of the evaporated water vapor progressively decreases. This decrease coincides with the apparition of back diffusion close to the surface, leading to the decrease of the soil surface liquid isotopic composition. This impoverishment of the isotopic composition of the evaporated water vapor increases as long as the soil dries. At the end of the experiment, a stabilization around a value of about –14 $^{o}/_{oo}$ can be observed.

3.4 Estimation of the isotopic composition of the evaporated water vapor

Table 6 provides the comparison between the measured and calculated (using Eq. (6)) oxygen 18 isotopic composition of the evaporated water vapor for various values of the kinetic fractionation factor. Figures 10 and 11 show the comparison of the estimated and measured values for α_K=1.0189 (laminar diffusion). Error bars on the estimation, as well as the minimum and maximum values estimated from Eq. (C.23 in Appendix C) are also provided. In Fig. 10, errors on the measured variables are assumed to be due to analytical or sensors accuracy only. In Fig. 11, sampling errors are considered. For both cases, the retained errors on the measured variables are given in Table 7.

Table 6 and Figs 10 and 11 show that, whatever the value retained for the kinetic fractionation factor, the calculated isotopic composition of the evaporated water vapor is much lower than the measured one. Figure 10 shows that analytical and sensors errors alone cannot explain this discrepancy as their use leads to very small standard errors. On the other hand, when sampling errors are considered (Fig. 11), the confidence intervals sometimes encompass the measured values. In the remaining of the paper, only standards errors calculated using

sampling errors will be presented, as they provide more realistic standard error values. Figure 12 provides the decomposition of the sources of errors, including (bottom) or excluding (top) errors on the kinetic fractionation factor. It shows that error on the isotopic composition of the soil surface liquid water is the major source of uncertainty in the estimation of the isotopic composition of the evaporated water using Eq. (6). Error on the soil surface water content becomes significant when the soil becomes very dry. When error on the kinetic fractionation factor is taken into account, it becomes the major source of uncertainty.

Table 6 and Figs 10 and 11 allow comparing the results for 6 dates with soil samples taken over different depths (grey lines). When the sampling depth is the smallest, the calculated isotopic composition of the evaporated water vapor is closer to the measured one before the apparition of the back diffusion (DoY 132, 154 and 192). In this case, a lower sampling depth is associated with a higher value of the soil isotopic ratio and to a higher value of the isotopic composition of the evaporated water (the partial derivative is positive under evaporation – see Eq. (C.20) in Appendix C). Therefore, when there is no back diffusion, the isotopic composition of the evaporated water seems to be controlled by the very soil surface isotopic ratio, which is difficult to sample. On the other hand, when back diffusion has taken place (DoY 264, 336, 439), the calculated isotopic composition of the evaporated water vapor is closer to the measured one when the thicker sampling depth is used. In case of back diffusion, the very soil surface isotopic composition of the liquid water does not seem to be the one controlling the isotopic composition of the evaporated water vapor, which appears to be related to the isotopic composition of the liquid water in deeper layers.

To investigate this point further, Table 8 provides the isotopic composition of the soil surface liquid water, given by Eq. (15), which would be required to match the measured and calculated values of the isotopic composition of the evaporated water. Results are provided for several values of the kinetic fractionation factor. The corresponding standard errors

(taking into account or not errors on the kinetic fractionation factor) are also given and the results are plotted in Fig. 13. Figure 14 shows the contribution of the various sources of errors to the total error. Table 8 shows that the calculated values for the isotopic composition of the soil liquid water are systematically higher than the values measured over the 0-2.5 or 0-0.5 cm depth, although the error bars encompass the measured values. The calculated values are close to the maximum value observed in the measured isotopic soil profiles (see Fig. 8 and Table 8), which corresponds to the evaporation front. The calculated values decrease when the kinetic fractionation factor decreases. Before the appearance of back diffusion (before DoY 193), the measured maximum are closer to the values calculated with the lowest kinetic fractionation factor value. After the appearance of back diffusion (after DoY 193), they are closer to values calculated with a kinetic fractionation factor of 1.0189. The standard error is generally between 2 and 4 $^{o}/_{oo}$, but increased up to 7-8 $^{o}/_{oo}$ when error on the kinetic fractionation factor is considered (Table 8). When the kinetic fractionation factor is not taken into account, the contribution of errors on the air and soil temperature, air relative humidity and isotopic composition of the evaporated water contribute equally well to the total error (see Fig. 14). Errors on the soil surface water content become significant when the soil is very dry. When error on the kinetic fractionation factor is included, Fig.14 shows that it has the same contribution as the other factors before the appearance of the water vapor back diffusion (before DoY 193). After this date, it becomes the major source of uncertainty.

The analysis presented in this section shows that the isotopic composition of the evaporated water vapor strongly depends on the soil isotopic composition of the soil liquid water. Before back diffusion, this isotopic composition seems to be controlled by the isotopic composition of the soil liquid water at the very surface. Such depth cannot be sampled up to now. When back diffusion has taken place, the picture still remains unclear. This point will be further analyzed in the companion paper using the modeling approach, especially to determine if a

relationship with the depth of the evaporating front (depth of the peak isotopic ratio in the soil) can be evidenced.

The results also suggest that the value of the kinetic fractionation factor which should be used in Eq. (6) is variable in time, with a notable difference before and after the appearance of back diffusion. This hypothesis is further examined in the following section where we try to estimate the value of the kinetic fractionation factor which ensures that measured and calculated (Eq. (6)) values of the isotopic composition of the evaporated water are equal. For this calculation the measured values (Table 4) of the isotopic composition of the soil surface liquid water were used, although the calculations performed in this section suggest that they might not be relevant all the time.

3.5 *Estimation of the kinetic fractionation factor*

Table 9 provides the values of the kinetic fractionation factor calculated using Eq. (16) for oxygen 18. It also provides estimates of the standard error, minimum and maximum estimated values using the method described in Appendix E, when considering sampling errors. Figure 15 gives the contribution of the various sources of errors to the total standard error. Table 9 shows that the calculation can lead to negative values of the kinetic fractionation factor, which is of course inconsistent with its definition. This result must be mitigated given the large uncertainty. Furthermore, the kinetic fractionation factor is an increasing function of the soil surface isotopic composition of water (Eq. E.12 in Appendix E). Therefore, the highest values of the soil surface isotopic ratio provide the highest estimates of the kinetic fractionation factor. Before the establishment of back diffusion (before DoY 193), the isotopic composition of the soil surface water is underestimated if thicker layers are taken into account (see also the comparison between the results for various depths in Table 9, grey lines). The best estimates of the kinetic fractionation factors would therefore be the upper bound of the estimation. After

the establishment of back diffusion (after DoY 193), the results are inverted, as also discussed in section 3.4. Higher values of the estimated kinetic fractionation factor are obtained when the soil surface isotopic ratio is estimated with thicker layers (grey lines in Table 9). The estimations of the kinetic fractionation factor provided in Table 9 are in general lower than the values commonly used in the literature (14 to 28.5 °/₀₀, Merlivat, 1978) for a free water surface, but the uncertainty is large. Figure 15 shows that the uncertainty on the isotopic composition of the soil liquid water is the major source of uncertainty in the calculation. After back diffusion (last three lines of Table 9), the kinetic fractionation factor was also estimated using the maximum values of soil water content and isotopic ratio encountered in the profile and corresponding to the evaporation front. In this case, the calculated values are well within the range of literature values (Merlivat, 1978) and confirms that, after back diffusion, the isotopic composition of the evaporated water vapor seems to be linked to the isotopic ratio at the evaporation front.

4. Conclusions

In Part I of this paper, we have presented a novel experiment which allows to measure simultaneously the evaporation flux and the isotopic composition of the evaporated water under controlled conditions for bare soil. We compared the measured isotopic composition of the evaporated water with traditional estimates. The results show that, using experimental data, none of the kinetic fractionation factor values encountered in the literature was able to give results in agreement with the measured ones. The error analysis also showed the high sensitivity of the results to the isotopic composition of the very soil surface liquid water. This raises question about the sampling depth required to get satisfactory results. Our results suggest that, when back diffusion has not occurred, the sampling depth should be as small as possible. On the other hand, when back diffusion has taken place (and the top soil profile

water movement takes place in the vapor phase), the isotopic composition of the evaporated water seems to be controlled by the value at the peak (evaporation front). If this results can be easily understood before back diffusion occurs, the relationship with the depth of the evaporation front requires further investigation. This is done in Part II of a companion paper (Braud et al., 2009) dedicated to the modeling of the experimental results using the SiSPAT_Isotope model of Braud et al. (2005a).

The data measured during the experiment allowed us to propose estimates of the kinetic fractionation factor of an evaporating soil. The uncertainty of the estimate is very large, as before, due to large uncertainties in the sampling depth required for the estimation of the isotopic composition of the soil liquid water. Although the average of the estimated values are lower than the values of Merlivat (1978) or Cappa et al. (2003) proposed in the literature and obtained for free surface water, results analysis suggest that a higher accuracy in the experimental design should be required to get a reliable estimate of the kinetic fractionation factor. Improvements must address the soil sampling to get a higher vertical resolution and also a better control of temperature in addition to the relative air humidity, so that the water vapor pressure, which controls the evaporation is more constant in time.

Acknowledgements

The "Programme National de Recherche en Hydrologie" of the French "ECosphère COntinentale" program is acknowledged for providing the financial support of the experiment.

Appendix A : Nomenclature of the variables used in the core of the paper (Appendices excluded)

DoD	Day of Drying
DoY	Day of the Year
e_{aout}	Water vapor pressure at the outlet of the column (Pa)
E	Water vapor or evaporation flux (kg m^{-2} s^{-1})
E_i	Isotopic water vapor flux at the surface (kg m^{-3})
g	Acceleration of gravity (m^2 s^{-1})

h	Soil water pressure (m)
$h_a^{'}$	Air relative humidity, normalized to the temperature of the water surface (-)
h_a	Air relative humidity (-)
h_s	Soil surface relative humidity (-)
M_i	Molar mass of the isotopic species (kg)
M_w	Molar mass ordinary water (kg)
P_{exp}	Pressure in the expansion fence (Pa)
q_{out}	Flow of water vapor at the outlet of the columns ($m^3\ s^{-1}$)
q_a	Air specific humidity ($kg\ kg^{-1}$)
q_s	(Soil) surface specific humidity ($kg\ kg^{-1}$)
r_a	Aerodynamic resistance to heat and water vapor transfer ($s\ m^{-1}$)
R	Perfect gas constant for vapor (461.5 $J\ kg^{-1}$)
R_i^l	Isotopic ratio in the liquid phase (-)
R_i^v	Isotopic ratio in the vapor phase (-)
R_{iE}^v	Isotopic ratio of the evaporated water vapor (-)
R_{is}^v	Isotopic ratio of the water vapor at the (soil) surface (-)
R_{ia}^v	Isotopic ratio of the water vapor in the atmosphere (-)
R_{iout}^v	Isotopic ratio of the water vapor at the outlet of the columns (-). In the context of the experiment, we have $R_{iout}^v = R_{ia}^v = R_{iE}^v$
R_{is}^l	Isotopic ratio of the liquid water at the (soil) surface (-)
S_{col}	Evaporative surface of the column (m^2)
T_a	Air temperature (K)
T_s	Surface temperature (K)
z	Depth within the soil column (positively oriented downwards) (m)
α_e	Equilibrium isotopic fractionation factor (-) $\alpha_e^* = 1/\alpha_e$
α_K	Isotopic kinetic fractionation factor (-)
δ_{iE}^v	Isotopic composition of the evaporated water vapor (delta)
δ_{is}^l	Isotopic composition of the (soil) surface liquid water (delta)
δ_{ia}^v	Isotopic composition of the ambient air water vapor (delta)
θ_{-i}	Volumetric water content at depth $-i$ ($m^3\ m^{-3}$)
θ_s	Volumetric water content at saturation ($m^3\ m^{-3}$)
ρ_a	Water vapor volumetric mass ($kg\ m^{-3}$)
$\rho_{sat}^v(T)$	Saturated volumetric mass of the water vapor ($kg\ m^{-3}$)
ΔS	Soil water storage variation (m)

Appendix B : Equations of the RUBIC IV reactor

Lets consider q_{in} ($m^3\ s^{-1}$) the incoming air flow, C_{in}^v ($kg\ m^{-3}$) its concentration in water vapor and $R_{i\_in}^v$ ($m^3\ s^{-1}$) its isotopic ratio. The notations are: q_{out}, C_{out}^v, and $R_{i\_out}^v$ for the air at the outlet of the column. Φ_{ev} ($kg\ s^{-1}$) is the water vapor flux released by the soil and R_{iE}^v its

isotopic ratio. V_c (m^3) is the air volume above the soil column, C^v_{col} (kg m^{-3}) its water vapor concentration and $R^v_{i\_col}$ its isotopic ratio.

The mass balance equation of the air above the soil column can be written as:

$$\frac{d\left(V_c C^v_{col}\right)}{dt} = q_{in} C^v_{in} + \phi_{ev} - q_{out} C^v_{out} \qquad \text{(B.1)}$$

Assuming that the reactor is a perfect mixing device and that the water vapor concentration above the column is instantaneously equal to that of the outlet vapor, i.e. $C^v_{col} = C^v_{out}$, Eq. (B.1) can be rewritten as:

$$\frac{dC^v_{out}}{C^v_{out} - \frac{q_{in} C^v_{in} + \phi_{ev}}{q_{out}}} = -\frac{q_{out} dt}{V_c} \qquad \text{(B.2)}$$

Considering that between t and $t + \Delta t$, q_{in}, q_{out} and Φ_{ev} fluxes are constant, the integration of the equation leads to:

$$C^v_{out} = \frac{q_{in} C^v_{in} + \phi_{ev}}{q_{out}} + \left(C^{v0}_{out} - \frac{q_{in} C^v_{in} + \phi_{ev}}{q_{out}} \right) \exp\left(-\frac{q_{out} \Delta t}{V_c} \right) \qquad \text{(B.3)}$$

where the ^{0} superscript refers to the value at time t.

The concentration at the outlet is measured and the unknown in Eq. (B.3) is the evaporation flux which is obtained by rearranging Eq. (B.3) as:

$$\phi_{ev} = q_{out} C^v_{out} \frac{1 - \frac{q_{in} C^v_{in}}{q_{out} C^v_{out}} - \left(\frac{C^{v0}_{vout}}{C^v_{out}} - \frac{q_{in} C^v_{in}}{q_{out} C^v_{out}} \right) \exp\left(-\frac{q_{out} \Delta t}{V_c} \right)}{1 - \exp\left(-\frac{q_{out} \Delta t}{V_c} \right)} \qquad \text{(B.4)}$$

Similar equations can be written for the isotopic species. They lead to:

$$\frac{d\left(V_c C^v_{col} R^v_{i\_col}\right)}{dt} = q_{in} C^v_{in} R^v_{i\_in} + \phi_{ev} R^v_{iE} - q_{out} C^v_{out} R^v_{i\_out} \qquad \text{(B.5)}$$

$$\frac{d\left(C_{out}^{v}R_{i\_out}^{v}\right)}{C_{out}^{v}R_{i\_out}^{v}-\frac{q_{in}C_{in}^{v}R_{i\_in}^{v}+\phi_{ev}R_{iE}^{v}}{q_{out}}}=-\frac{q_{out}dt}{V_c} \qquad \text{(B.6)}$$

$$C_{out}^{v}R_{i\_out}^{v}=\frac{q_{in}C_{in}^{v}R_{i\_in}^{v}+\phi_{ev}R_{iE}^{v}}{q_{out}}+\left(C_{vout}^{v0}R_{i\_out}^{v0}-\frac{q_{in}C_{in}^{v}R_{i\_in}^{v}+\phi_{ev}R_{iE}^{v}}{q_{out}}\right)\exp\left(-\frac{q_{out}\Delta t}{V_c}\right) \qquad \text{(B.7)}$$

$$\phi_{ev}R_{iE}^{v}=q_{out}C_{out}^{v}R_{i\_out}^{v}\frac{1-\frac{q_{in}C_{in}^{v}R_{i\_in}^{v}}{q_{out}C_{out}^{v}R_{i\_out}^{v}}-\left(\frac{C_{vout}^{v0}R_{vout}^{v0}}{C_{vout}^{v0}R_{vout}^{v0}}-\frac{q_{in}C_{in}^{v}R_{i\_in}^{v}}{q_{out}C_{out}^{v}R_{i\_out}^{v}}\right)\exp\left(-\frac{q_{out}\Delta t}{V_c}\right)}{1-\exp\left(-\frac{q_{out}\Delta t}{V_c}\right)} \qquad \text{(B.8)}$$

In Eqs (B.4) and (B.8), the $\exp\left(-\frac{q_{out}\Delta t}{V_c}\right)$ term takes into account a possible inertia of the reactor in transmitting the evaporation flux towards the outlet.

With the experimental conditions prevailing in the reactor, the incoming air was dry, therefore C_{in}^{v}=0. The air volume above the column was $V_c=\pi R^2 H=1.131\ 10^{-3}\ m^3$, with R = 0.06 m for the radius and H = 0.1 m for the height above the soil surface. The integration time was Δt=900 s, q_{out} was ranging between 0.5 and 0.15 l min^{-1}, i.e. 8.33 and 2.5 10^{-6} m^3 s^{-1}.

Therefore the exponential term $\exp\left(-\frac{q_{out}\Delta t}{V_c}\right)$ was ranging between 1.32 10^{-3} at the beginning of the experiment to 0.137 at the end. The calculation of the evaporation flux with Eq. (B.4) showed that the correction was negligible with a difference in cumulated evaporation of less than 0.1 mm.

For the isotopic trapping, the time step was Δt=86400 s, therefore the same exponential term was close to zero. Therefore, for the conditions of the experiment, the following approximations:

$$\phi_{ev}=q_{out}C_{out}^{v} \qquad \text{(A.9)} \qquad \text{and} \qquad R_{iE}^{v}=R_{out}^{v} \qquad \text{(B.10)}$$

were valid and have been used in the data analysis.

Appendix C: Derivation of standard error for the estimated isotopic composition of the evaporated water vapor

The isotopic composition of the evaporated water vapor is given by Eq. (6)

$$R_{iE}^{v} = \frac{1}{\alpha_K}\frac{\left(\alpha_e^* R_{is}^{l} h_s - R_{ia}^{v} h_a^{'}\right)}{\left(h_s - h_a^{'}\right)} \quad \text{(C.1)}$$

with $R_{ia}^{v} = R_{iout}^{v}$ in the context of the experiment. The standard error can be obtained using an extension of the formula proposed by Phillips and Gregg (2001). The result of Eq. (C.1) depends on errors on the measurements of the air temperature and humidity T_a and h_a, the soil temperature T_s, the soil surface water content θ, the isotopic composition of the soil surface liquid water δ_{is}^{l} and of the water vapor above the soil column δ_{ia}^{v}. We can also take into account the error on the kinetic fractionation factor α_K (last term in parentheses in Eq. (C.2)). Assuming that the errors on all these factors are independent, the standard error $\sigma_{R_{iE}^{v}}$ can be expressed as:

$$\sigma_{R_{iE}^{v}}^{2} = \left(\frac{\partial R_{iE}^{v}}{\partial T_s}\right)^2 \sigma_{T_s}^2 + \left(\frac{\partial R_{iE}^{v}}{\partial T_a}\right)^2 \sigma_{T_a}^2 + \left(\frac{\partial R_{iE}^{v}}{\partial h_a}\right)^2 \sigma_{ha}^2 + \left(\frac{\partial R_{iE}^{v}}{\partial \delta_{is}^{l}}\right)^2 \sigma_{\delta_{is}^{l}}^2 + \left(\frac{\partial R_{iE}^{v}}{\partial \delta_{ia}^{v}}\right)^2 \sigma_{\delta_{ia}^{v}}^2 + \left(\frac{\partial R_{iE}^{v}}{\partial \theta}\right)^2 \sigma_{\theta}^2 + \left(\left(\frac{\partial R_{iE}^{v}}{\partial \alpha_K}\right)^2 \sigma_{\alpha_K}^2\right) \quad \text{(C.2)}$$

The partial derivatives of Eq. (C.2) can be obtained using the chain rules:

$$\frac{\partial R_{iE}^{v}}{\partial T_s} = \frac{\partial R_{iE}^{v}}{\partial \alpha_e^*}\frac{\partial \alpha_e^*}{\partial T_s} + \frac{\partial R_{iE}^{v}}{\partial h_a^{'}}\frac{\partial h_a^{'}}{\partial T_s} \quad \text{(C.3)} \qquad \frac{\partial R_{iE}^{v}}{\partial T_a} = \frac{\partial R_{iE}^{v}}{\partial h_a^{'}}\frac{\partial h_a^{'}}{\partial T_a} \quad \text{(C.4)}$$

$$\frac{\partial R_{iE}^{v}}{\partial h_a} = \frac{\partial R_{iE}^{v}}{\partial h_a^{'}}\frac{\partial h_a^{'}}{\partial h_a} \quad \text{(C.5)} \qquad \frac{\partial R_{iE}^{v}}{\partial \delta_{is}^{l}} = \frac{\partial R_{iE}^{v}}{\partial R_{is}^{l}}\frac{\partial R_{is}^{l}}{\partial \delta_{is}^{l}} \quad \text{(C.6)}$$

$$\frac{\partial R_{iE}^{v}}{\partial \delta_{ia}^{v}} = \frac{\partial R_{iE}^{v}}{\partial R_{ia}^{v}}\frac{\partial R_{ia}^{v}}{\partial \delta_{ia}^{v}} \quad \text{(C.7)} \qquad \frac{\partial R_{iE}^{v}}{\partial \theta} = \frac{\partial R_{iE}^{v}}{\partial h_s}\frac{\partial h_s}{\partial h}\frac{\partial h}{\partial \theta} \quad \text{(C.8)}$$

The partial derivatives appearing in these expressions are given below:

$$\frac{\partial R_{iE}^{v}}{\partial \alpha_{e}^{*}} = \frac{1}{\alpha_K} \frac{R_{is}^{l} h_s}{\left(h_s - h_a^{'}\right)} \quad \text{(C.9)} \qquad \frac{\partial \alpha_{e}^{*}}{\partial T_s} = \alpha_{e}^{*}\left(\frac{2a}{T_s^3} + \frac{b}{T_s^2}\right) \quad \text{(C.10)}$$

$$\alpha_{e}^{*}\left(T_s\right) = \exp\left(-\left[\frac{a}{T_s^2} + \frac{b}{T_s} + c\right]\right) \quad \text{(C.11)}$$

with:

$$\begin{cases} a = 1137. \\ b = -0.4156 \\ c = -0.0020667 \end{cases} \quad \text{for } H_2{}^{18}O$$

$$\frac{\partial R_{iE}^{v}}{\partial h_a^{'}} = \frac{1}{\alpha_K} \frac{\left(\alpha_{e}^{*} R_{is}^{l} - R_{ia}^{v}\right) h_s}{\left(h_s - h_a^{'}\right)^2} \quad \text{(C.12)} \qquad \frac{\partial h_a^{'}}{\partial T_s} = h_a^{'}\left(\frac{1}{T_s} - \frac{1}{e_{sat}\left(T_s\right)} \frac{de_{sat}\left(T_s\right)}{dT_s}\right) \quad \text{(C.13)}$$

$$\frac{\partial h_a^{'}}{\partial T_a} = -h_a^{'}\left(\frac{1}{T_a} - \frac{1}{e_{sat}\left(T_a\right)} \frac{de_{sat}\left(T_a\right)}{dT_a}\right) \quad \text{(C.14)} \qquad \frac{\partial h_a^{'}}{\partial h_a} = \frac{h_a^{'}}{h_a} \quad \text{(C.15)}$$

$$\frac{\partial R_{iE}^{v}}{\partial h_s} = -\frac{1}{\alpha_K} \frac{\left(\alpha_{e}^{*} R_{is}^{l} - R_{ia}^{v}\right) h_a^{'}}{\left(h_s - h_a^{'}\right)^2} \quad \text{(C.16)} \qquad \frac{\partial h_s}{\partial h} = \frac{g h_s}{R T_s} \quad \text{(C.17)}$$

$$\frac{\partial h}{\partial \theta} = \frac{h_g}{mn\theta_s}\left(\frac{\theta}{\theta_s}\right)^{\left(-\frac{1}{m}-1\right)}\left[\left(\frac{\theta}{\theta_s}\right)^{-\frac{1}{m}} - 1\right]^{\left(\frac{1}{n}-1\right)} \quad \text{(C.18) with} \quad h = h_g\left[\left(\frac{\theta}{\theta_s}\right)^{-\frac{1}{m}} - 1\right]^{\frac{1}{n}} \quad \text{(C.19)}$$

$$\frac{\partial R_{iE}^{v}}{\partial \delta_{is}^{l}} = \frac{\partial R_{iE}^{v}}{\partial R_{is}^{l}} \frac{\partial R_{is}^{l}}{\partial \delta_{is}^{l}} = \frac{1}{\alpha_K} \frac{\alpha_{e}^{*} h_s}{\left(h_s - h_a^{'}\right)} \frac{R_{ref}}{1000} \quad \text{(C.20)}$$

$$\frac{\partial R_{iE}^{v}}{\partial \delta_{ia}^{v}} = \frac{\partial R_{iE}^{v}}{\partial R_{ia}^{v}} \frac{\partial R_{ia}^{v}}{\partial \delta_{ia}^{v}} = -\frac{1}{\alpha_K} \frac{h_a^{'}}{\left(h_s - h_a^{'}\right)} \frac{R_{ref}}{1000} \quad \text{(C.21)}$$

where R_{ref} are the reference values for the isotopic ratio ($2005.2\ 10^{-6}$ for $H_2{}^{18}O$)

$$\frac{\partial R_{iE}^{v}}{\partial \alpha_K} = -\frac{R_{iE}^{v}}{\alpha_K} \quad \text{(C.22)}$$

We also estimated the standard error using a more empirical method by deriving a series of estimation of the water vapor isotopic composition and by combining all the possibilities with

+ or – standard errors on all the variables (64 combinations with 6 variables) using Eq. (C.23).

$$\Delta R_{iE}^{v} = \left(\frac{\partial R_{iE}^{v}}{\partial T_s}\right)_{T_s}\left(\pm \Delta T_s\right) + \left(\frac{\partial R_{iE}^{v}}{\partial T_a}\right)_{T_a}\left(\pm \Delta T_a\right) + \left(\frac{\partial R_{iE}^{v}}{\partial h_a}\right)_{h_a}\left(\pm \Delta h_a\right) + \left(\frac{\partial R_{iE}^{v}}{\partial \delta_{is}^{l}}\right)_{\delta_{is}^{l}}\left(\pm \Delta \delta_{is}^{l}\right) + \left(\frac{\partial R_{iE}^{v}}{\partial \delta_{ia}^{v}}\right)_{\delta_{ia}^{v}}\left(\pm \Delta \delta_{ia}^{v}\right) + \left(\frac{\partial R_{iE}^{v}}{\partial \theta}\right)_{\theta}\left(\pm \Delta \theta\right) \quad \text{(C.23)}$$

We checked that the standard deviation of the corresponding series was equal to the standard error given by Eq. (C.2 in Appendix C). With this method we were able to get minimum and maximum values for the estimation of the composition of the soil evaporation and to know which combinations of errors were leading to values closer to the observations.

Appendix D: Derivation of standard error for the estimated isotopic composition of the soil liquid water which matches the observed isotopic composition of the evaporated water vapor. The corresponding value is given by Eq. (15)

$$R_{is}^{l} = \frac{R_{iout}^{v}\left(h_s\alpha_K - h_a^{'}\left(\alpha_K - 1\right)\right)}{\alpha_e^{*} h_s} \quad \text{(D.1)}$$

The standard error can be obtained using an extension of the formula proposed by Phillips and Gregg (2001). The result of Eq. (D.1) depends on errors on the measurements of air temperature and humidity T_a and h_a, the soil temperature T_s, the soil surface water content θ, and of the water vapor above the soil column, equal to that at the outlet of the column δ_{iout}^{v}. We assume that the errors on all these factors are independent. Thus the standard error $\sigma_{R_{is}^{l}}$ can be obtained as:

$$\sigma_{R_{is}^{l}}^{2} = \left(\frac{\partial R_{is}^{l}}{\partial T_s}\right)^2 \sigma_{T_s}^{2} + \left(\frac{\partial R_{is}^{l}}{\partial T_a}\right)^2 \sigma_{T_a}^{2} + \left(\frac{\partial R_{is}^{l}}{\partial h_a}\right)^2 \sigma_{ha}^{2} + \left(\frac{\partial R_{is}^{l}}{\partial \delta_{iout}^{v}}\right)^2 \sigma_{\delta_{iout}^{v}}^{2} + \left(\frac{\partial R_{is}^{l}}{\partial \theta}\right)^2 \sigma_{\theta}^{2} + \left(\frac{\partial R_{is}^{l}}{\partial \alpha_K}\right)^2 \sigma_{\alpha_K}^{2} \quad \text{(D.2)}$$

The partial derivatives of Eq. (D.2.) can be obtained using the chain rules:

$$\frac{\partial R_{is}^{l}}{\partial T_s}=\frac{\partial \alpha_K}{\partial \alpha_e^{*}}\frac{\partial \alpha_e^{*}}{\partial T_s}+\frac{\partial R_{is}^{l}}{\partial h_a^{'}}\frac{\partial h_a^{'}}{\partial T_s} \quad \text{(D.3)} \qquad \frac{\partial R_{is}^{l}}{\partial T_a}=\frac{\partial R_{is}^{l}}{\partial h_a^{'}}\frac{\partial h_a^{'}}{\partial T_a} \quad \text{(D.4)}$$

$$\frac{\partial R_{is}^{l}}{\partial h_a}=\frac{\partial R_{is}^{l}}{\partial h_a^{'}}\frac{\partial h_a^{'}}{\partial h_a} \quad \text{(D.5)} \qquad \frac{\partial R_{is}^{l}}{\partial \delta_{iout}^{v}}=\frac{\partial R_{is}^{l}}{\partial R_{iout}^{v}}\frac{\partial R_{iout}^{v}}{\partial \delta_{iout}^{v}} \quad \text{(D.6)}$$

$$\frac{\partial R_{is}^{l}}{\partial \theta}=\frac{\partial R_{is}^{l}}{\partial h_s}\frac{\partial h_s}{\partial h}\frac{\partial h}{\partial \theta} \quad \text{(D.7)} \qquad \frac{\partial R_{is}^{l}}{\partial \alpha_K}=\frac{R_{iout}^{v}\left(h_s-h_a^{'}\right)}{\alpha_e^{*}h_s} \quad \text{(D.8)}$$

The partial derivatives appearing in these expressions, not already provided in Appendix C, are given below:

$$\frac{\partial R_{is}^{l}}{\partial \alpha_e^{*}}=-\frac{R_{iout}^{v}\left(\alpha_K h_s-h_a^{'}\left(\alpha_K-1\right)\right)}{\alpha_e^{*2}h_s}=-\frac{R_{is}^{l}}{\alpha_e^{*}} \quad \text{(D.9)}$$

$$\frac{\partial R_{is}^{l}}{\partial h_a^{'}}=-\frac{R_{iout}^{v}\left(\alpha_K-1\right)}{\alpha_e^{*}h_s} \quad \text{(D.10)} \qquad \frac{\partial R_{is}^{l}}{\partial h_s}=\frac{R_{iout}^{v}h_a^{'}\left(\alpha_K-1\right)}{\alpha_e^{*}h_s^{\,2}} \quad \text{(D.11)}$$

$$\frac{\partial R_{is}^{l}}{\partial \delta_{iout}^{v}}=\frac{\partial R_{is}^{l}}{\partial R_{iout}^{v}}\frac{\partial R_{iout}^{v}}{\partial \delta_{ia}^{v}}=\frac{\left(h_s\alpha_K-h_a^{'}\left(\alpha_K-1\right)\right)}{\alpha_e^{*}h_s}\frac{R_{ref}}{1000} \quad \text{(D.12)}$$

As in Appendix C, we also derived an empirical estimation of the error using the following equation:

$$\Delta R_{is}^{l}=\left(\frac{\partial R_{is}^{l}}{\partial T_s}\right)_{T_s}\left(\pm\Delta T_s\right)+\left(\frac{\partial R_{is}^{l}}{\partial T_a}\right)_{T_a}\left(\pm\Delta T_a\right)+\left(\frac{\partial R_{is}^{l}}{\partial h_a}\right)_{h_a}\left(\pm\Delta h_a\right)+\left(\frac{\partial R_{is}^{l}}{\partial \delta_{iout}^{v}}\right)_{\delta_{iout}^{v}}\left(\pm\Delta\delta_{iout}^{v}\right)+$$
$$+\left(\frac{\partial R_{is}^{l}}{\partial \theta}\right)_{\theta}\left(\pm\Delta\theta\right)+\left(\frac{\partial R_{is}^{l}}{\partial \alpha_K}\right)_{\delta_{is}^{l}}\left(\pm\Delta\alpha_K\right) \quad \text{(D.13)}$$

Appendix E: Derivation of standard error for the estimated kinetic fractionation factor using Eq. (16)

The kinetic fractionation factor is given by Eq. (16)

$$\alpha_K=\frac{\left(\alpha_e^{*}R_{is}^{l}h_s-R_{iout}^{v}h_a^{'}\right)}{\left(h_s-h_a^{'}\right)R_{iout}^{v}} \quad \text{(E.1)}$$

The standard error can be obtained using an extension of the formula proposed by Phillips and Gregg (2001). The result of Eq. (E.1) depends on errors on the measurements of air temperature and humidity T_a and h_a, the soil temperature T_s, the soil surface water content θ, the isotopic composition of the soil surface liquid water δ_{is}^{l} and of the water vapor above the soil column, equal to that at the outlet of the column δ_{iout}^{v}. We assume that the errors on all these factors are independent. Thus the standard error σ_{α_K} can be obtained as:

$$\sigma_{\alpha_K}^2 = \left(\frac{\partial \alpha_K}{\partial T_s}\right)^2 \sigma_{T_s}^2 + \left(\frac{\partial \alpha_K}{\partial T_a}\right)^2 \sigma_{T_a}^2 + \left(\frac{\partial \alpha_K}{\partial h_a}\right)^2 \sigma_{ha}^2 + \left(\frac{\partial \alpha_K}{\partial \delta_{is}^{l}}\right)^2 \sigma_{\delta_{is}^{l}}^2 + \left(\frac{\partial \alpha_K}{\partial \delta_{iout}^{v}}\right)^2 \sigma_{\delta_{iout}^{v}}^2 + \left(\frac{\partial \alpha_K}{\partial \theta}\right)^2 \sigma_{\theta}^2 \quad \text{(E.2)}$$

The partial derivatives of Eq. (E.2) can be obtained using the chain rules:

$$\frac{\partial \alpha_K}{\partial T_s} = \frac{\partial \alpha_K}{\partial \alpha_e^*}\frac{\partial \alpha_e^*}{\partial T_s} + \frac{\partial \alpha_K}{\partial h_a^{'}}\frac{\partial h_a^{'}}{\partial T_s} \quad \text{(E.3)} \qquad \frac{\partial \alpha_K}{\partial T_a} = \frac{\partial \alpha_K}{\partial h_a^{'}}\frac{\partial h_a^{'}}{\partial T_a} \quad \text{(E.4)}$$

$$\frac{\partial \alpha_K}{\partial h_a} = \frac{\partial \alpha_K}{\partial h_a^{'}}\frac{\partial h_a^{'}}{\partial h_a} \quad \text{(E.5)} \qquad \frac{\partial \alpha_K}{\partial \delta_{is}^{l}} = \frac{\partial \alpha_K}{\partial R_{is}^{l}}\frac{\partial R_{is}^{l}}{\partial \delta_{is}^{l}} \quad \text{(E.6)}$$

$$\frac{\partial \alpha_K}{\partial \delta_{iout}^{v}} = \frac{\partial \alpha_K}{\partial R_{iout}^{v}}\frac{\partial R_{iout}^{v}}{\partial \delta_{iout}^{v}} \quad \text{(E.7)} \qquad \frac{\partial \alpha_K}{\partial \theta} = \frac{\partial \alpha_K}{\partial h_s}\frac{\partial h_s}{\partial h}\frac{\partial h}{\partial \theta} \quad \text{(E.8)}$$

The partial derivatives appearing in these expressions, not already provided in Appendix C, are given below:

$$\frac{\partial \alpha_K}{\partial \alpha_e^*} = \frac{R_{is}^{l} h_s}{R_{iout}^{v}\left(h_s - h_a^{'}\right)} \quad \text{(E.9)} \qquad \frac{\partial \alpha_K}{\partial h_a^{'}} = \frac{\left(\alpha_e^* R_{is}^{l} - R_{iout}^{v}\right)h_s}{R_{iout}^{v}\left(h_s - h_a^{'}\right)^2} \quad \text{(E.10)}$$

$$\frac{\partial \alpha_K}{\partial h_s} = -\frac{\left(\alpha_e^* R_{is}^{l} - R_{iout}^{v}\right)h_a^{'}}{R_{iout}^{v}\left(h_s - h_a^{'}\right)^2} \quad \text{(E.11)} \qquad \frac{\partial \alpha_K}{\partial \delta_{is}^{l}} = \frac{\partial \alpha_K}{\partial R_{is}^{l}}\frac{\partial R_{is}^{l}}{\partial \delta_{is}^{l}} = \frac{\alpha_e^* h_s}{R_{iout}^{v}\left(h_s - h_a^{'}\right)}\frac{R_{ref}}{1000} \quad \text{(E.12)}$$

$$\frac{\partial \alpha_K}{\partial \delta_{iout}^{v}} = \frac{\partial \alpha_K}{\partial R_{iout}^{v}}\frac{\partial R_{iout}^{v}}{\partial \delta_{ia}^{v}} = -\frac{h_s \alpha_e^* R_{is}^{l}}{\left(R_{iout}^{v}\right)^2\left(h_s - h_a^{'}\right)}\frac{R_{ref}}{1000} \quad \text{(E.13)}$$

As in Appendix C, we also derived an empirical estimation of the error using the following equation:

$$\Delta\alpha_K = \left(\frac{\partial\alpha_K}{\partial T_s}\right)_{T_s}\left(\pm\Delta T_s\right)+\left(\frac{\partial\alpha_K}{\partial T_a}\right)_{T_a}\left(\pm\Delta T_a\right)+\left(\frac{\partial\alpha_K}{\partial h_a}\right)_{h_a}\left(\pm\Delta h_a\right)+\left(\frac{\partial\alpha_K}{\partial\delta_{is}^l}\right)_{\delta_{is}^l}\left(\pm\Delta\delta_{is}^l\right)+ \\ +\left(\frac{\partial\alpha_K}{\partial\delta_{iout}^v}\right)_{\delta_{iout}^v}\left(\pm\Delta\delta_{iout}^v\right)+\left(\frac{\partial\alpha_K}{\partial\theta}\right)_{\theta}\left(\pm\Delta\theta\right) \tag{E.14}$$

References

Araguás-Araguás, L., Rozanski, K., Gonfiantini, R., Louvat, D., 1995. Isotope effects accompanying vacuum extraction of soil water for stable isotope analyses. J.Hydrol. 168, 159-171.

Bariac, T., Gonzalez-Dunia, J., Katerji, N., Béthenod, O., Bertolini, J.M., Mariotti, A., 1994. Variabilité spatio-temporelle de la composition isotopique de l'eau (18O, 2H) dans le continuum sol-plante-atmosphère : 2. Approche en conditions naturelles. Chem. Geol. 115(3-4), 317-333.

Barnes, C.J., Allison, G.B., 1983. The distribution of deuterium and 18O in dry soils: 1. Theory. J. Hydrol. 60, 141-156.

Barnes, C.J., Allison, G.B., 1984. The distribution of D and 18O in dry soils. 3- Theory for non-isothermal water movement. J. Hydrol. 74, 119-135.

Braud, I., Bariac, T., Biron, Ph., Vauclin, M., 2009. Isotopic composition of bare soil evaporated water vapor. Part II: Modelling of RUBIC IV experimental results. J. Hydrol., submitted.

Braud, I., Bariac, T., Gaudet, J.P., Vauclin, M., 2005a. SiSPAT-Isotope , a coupled heat, water and stable isotope (HDO and H218O) transport model for bare soil. Model description and first verification. J. Hydrol. 309(1-4), 277-300.

Braud, I., Bariac, T., Vauclin, M., Boujamlaoui, Z., Gaudet, J.P., Biron, P., Richard, P., 2005b. SiSPAT-Isotope , a coupled heat, water and stable isotope (HDO and H218O) transport model for bare soil. Evaluation and sensitivity tests using two laboratory data sets. J. Hydrol. 309(1-4), 301-320.

Cappa, C.D., Hendricks, M.B., DePaolo, D.J., Cohen, R.C., 2003. Isotopic fractionation of water during evaporation. J. Geophys. Res. 108(D16), 4525, doi:10.1029/2003JD003597.

Chahine, M. T. (1992). The hydrological cycle and its influence on climate. Nature 359, 373-380.

Costanza, R. et al.. 1997. The value of the world's ecosytems services and natural capital. Nature 387, 253-260.

Craig, H., Gordon, L.I., 1965. Deuterium and oxygen 18 variations in the ocean and the marine atmosphere, Proceedings of the Conference on the stable isotopes in oceanographic studies and paleotemperatures, Lab. Geol. Nucl., Pisa, Italy, 9-130.

Dongmann, G., Nürnberg, H.W., 1974. On the enrichment of H218O in the leaves of transpiring plants. Rad. and Environm. Biophys. 11, 41-52.

Gonfiantini, R., 1978. Standards for stable isotope measurements in natural compounds. Nature 271, 534-536.

Majoube, M.A., 1971. Fractionnement en oxygène-18 et en deutérium entre l'eau et sa vapeur, J. Chem. Phys. 68, 1423-1436.

Merlivat, L., 1978. Molecular diffusivity of H216O, HD16O and H218O in gases. J. Chem. Physics 69(6), 2864-2871.

Merlivat, L., Jouzel, J., 1979. Global climatic interpretation of the Deuterium-Oxygen 18 relationship for precipitation. J. Geophys. Res. 84(C8), 5029-5033.

Parlange M.B., Katul G.G., 1992, Estimation of the diurnal variation of potential evaporation from a wet bare soil surface, J. Hydrol. 132, 71-89.

Phillips, D.L., Gregg, J.W., 2001. Uncertainty in source partitioning using stable isotopes. Oecologia 127, 171-179.

Schoch-Fischer H., Rozanski K., Jacob H., Sonntag C., Jouzel J., Ostlund G., Geyh M.A.. 1983. Hydrometeorological factors controlling the time variation of D, ^{18}O and ^{3}H in atmospheric water vapour and precipitation in the northwestern westwind belt. *In* Proc. Symp. Vienna, 12-16 september 1983, AIEA-UNESCO, *Isotope Hydrology*: Vienna; 3-30.

Van Genuchten, M.T., 1980. A closed-form equation for predicting the hydraulic conductivity of unsaturated soils. Soil Sci. Soc.Am. J. 44, 892-898.

Walker, C.D., Richardson, S.B., 1991. The use of stable isotopes of water in characterizing the sources of water in vegetation. Chem. Geol. (Iso. Geo. Sect.) 94, 145-158.

Williams, D.G., Cable, W., Hultine, K., Hoedjes, J.C.B., Yepez, E.A., Simmoneaux, V., Er-Raki, S., Boulet, G., de Bruin, H.A.R., Cheehbouni, A., Hartogensis, O.K., Timouk, F., 2004. Evapotranspiration components determined by stable isotope, sap flow and eddy covariance techniques. Agricul. For. Meteorol. 125, 241-258.

Yakir, D., da Silveira Lobo Sternberg, L., 2000. The use of stable isotopes to study ecosystem gas exchange. Oecologia 123, 297-311.

Yepez, E.A., Williams, D.G., Scott, R.L., Lin, G., 2003. Partitioning overstory and understory evapotranspiration in a semiarid savanna woodland from the isotopic composition of water vapor. Agricul. For. Meteorol. 119(1-2), 53-68.

Zangvil, A., Portis, D.H., Lamb, P.J., 2004. Investigation of the large scale atmospheric moisture field over the Midwestern United States in relation to summer precipitation. Part II: Recycling of local evapotranspiration and association with soil moisture and crop yields. J. Climate 17, 3283-3301.

Zimmermann U., Ehhalt D., Münnich K.O., 1967. Soil - water movement and evapotranspiration: changes in the isotopic composition of the water. Proc. Symp. Isot. Hydrol., Vienna, I. A. E. A., pp 567-584.

List of figures

Figure 1. Photo of the experimental set up.

Figure 2. Scheme of the experimental set up (view from the top).

Figure 3: Time evolution of air temperature and relative humidity at the outlet of column 1.

Figure 4. Evolution of the oxygen 18 composition of the liquid water as function of the gravimetric water content (kg kg^{-1}). The results were obtained after 15h of distillation and corrected for the efficiency of the extraction. The target initial oxygen 18 isotopic composition of the liquid water is -7.10 ± 0.05 °/∞. Vertical bars correspond to the analytical errors (± 0.1 °/∞).

Figure 5. Retention curve $h(\theta)$ of the soil. The squares correspond to the measured (h,θ) couples at –2.5 cm (full square), -8 cm (crosses), -16 cm (open triangles). The continuous line corresponds to the fitted Van Genuchten model $\frac{\theta}{\theta_{sat}} = \left(1+\left(\frac{h}{h_{VG}}\right)^{n}\right)^{-m}$ *with* $m = 1-\frac{2}{n}$ for the -2.5 cm data. Values of the parameters are n=2.36, h_{VG}=-1.05 m, θ_{sat}=0.444.

Figure 6. Comparison of the cumulative evaporation (left) and the instantaneous flux (right) estimated by using the measures of air flow and water vapor humidity at the outlet (full black), the weighting of the columns (dashed black), the trapped water volume at the outlet (dashed light) and the calculated soil water storage (full light) for column 1 (top) and column 4 (bottom).

Figure 7. Evaporation flux of the six columns (top) and cumulative evaporation of the six columns (bottom). Values were calculated using Method 1.

Figure 8. Volumetric water content (left) and oxygen 18 isotopic ratio (right) (in °/∞) of the six soil columns when they were dismantled. The vertical straight lines are the initial values. DoY is Day of the Year

Figure 9. Time evolution of the oxygen 18 isotopic ratio of the evaporated water vapor for the six columns. The horizontal black line gives the composition of the initial water –6.4 °/∞. The sampling frequency is twice a day from DoY 101 to 136; once a day from DoY 137 to 224 and then about one sample every two or three days.

Figure 10. Comparison of the measured oxygen 18 composition of the evaporated water vapor (squares) and the calculated one using Eq. (6) with α_K=1.0189 (points). Values of the standard error, as well as their minimum and maximum, estimated using analytical and sensor accuracy errors are also plotted. Results with soil water content and liquid isotopic ratios sampled over the 0-2.5 cm and 0-0.5 or 0-1 cm layers are represented in the top and bottom panels, respectively.

Figure 11. Comparison of the measured oxygen 18 composition of the evaporated water vapour (squares) and the calculated one using Eq. (6) with α_K=1.0189 (points). Values of the standard error, as well as their minimum and maximum, estimated using sampling errors are plotted. Results with soil water content and liquid isotopic ratios sampled over the 0-2.5 cm and 0-0.5 or 0-1 cm layers are represented in the top and bottom panels, respectively.

Figure 12. Contribution of the various sources of errors on the calculated isotopic composition of the evaporated water vapor for oxygen 18 for the sampling errors and α_K=1.0189. Top panel: when error on α_K is not taken into account. Bottom panel: when error on α_K is taken into account. The dates in abscissa correspond to the lines in Table 6 in the same order. In the legend, the labels refer to errors on soil temperature T_s (Ts), isotopic composition of the soil surface liquid water δ_{is}^{l} (deltal), water vapor above the soil column δ_{ia}^{v} (deltair), air temperature T_a (Ta), air relative humidity h_a (ha), soil water content θ (theta) and kinetic fractionation factor α_K (alphak).

Figure 13. Value of the isotopic composition of the soil liquid water, required so that the isotopic composition of the evaporated water vapor calculated using Eq. (6) matches the measured value. The standard error, minimum and maximum values estimated using sampling errors are also plotted. Measured values correspond to the 0-2.5 cm depth layer.

Figure 14 Contribution of the various sources of errors on the calculated isotopic composition of the soil liquid water required so that the isotopic composition of the evaporated water vapor calculated using Eq. (6) matches the measured value calculated using oxygen 18 and the sampling errors. Top: error on the kinetic fractionation factor is not considered. Bottom: Error on the kinetic fractionation factor is considered. The dates in abscissa correspond to the lines in Table 8 in the same order. In the legend the labels refer to errors on soil temperature T_s (Ts), water vapor above the soil column δ_{ia}^{v} (deltair), air temperature T_a (Ta), air relative humidity h_a (ha), soil water content θ (theta) and kinetic fractionation factor α_K (alphak).

Figure 15. Contribution of the various sources of errors on the calculated kinetic fractionation factor for oxygen 18 and for the sampling errors. The dates in abscissa correspond to the lines in Table 9 in the same order. In the legend the labels refer to errors on soil temperature T_s (Ts), isotopic composition of the soil surface liquid water δ_{is}^{l} (deltal), water vapor above the soil column δ_{ia}^{v} (deltair), air temperature T_a (Ta), air relative humidity h_a (ha), soil water content θ (theta).

1 Table 1 Dates and values at which the constraint on the relative humidity above the soil
2 column was modified

Date of change of the prescribed relative humidity	Corresponding Day of the Year	Time since beginning of simulation (s)	Value of the prescribed relative humidity (-)
April 11 2005 12h00	DoY 101 12h00	0	0.8
July 25 2005 16h45	DoY 207 16h45	$9.1735\ 10^{6}$	0.6
August 28 2005 15h00	DoY 241 15h00	$1.21068\ 10^{7}$	0.5
September 26 2005 12h45	DoY 269 12h45	$1.45179\ 10^{7}$	0.4
October 14 2005 16h15	DoY 287 16h15	$1.60857\ 10^{7}$	0.3
November 2 2005 12h00	DoY 306 12h00	$1.7712\ 10^{7}$	0.2

3

1 Table 2 Initial weight, moisture and isotopic conditions of the six columns

	Column 6	Column 5	Column 3	Column 2	Column 4	Column 1
Soil Volume (cm^3)	3958	3958	3958	3958	3958	3971
Dry soil mass (g)	5603	5698	5456	5470	5580	5661
Water mass for the saturation of the soil (g)	1678	1742	1724	1717	1691	1728
Saturated water content[(a)] ($m^3\ m^{-3}$)	0.42	0.44	0.44	0.43	0.43	0.44
Dry bulk density[(b)] ($g\ cm^{-3}$)	1.42	1.44	1.38	1.38	1.41	1.44
Isotopic concentration in $H_2{}^{18}O$ of the initial water at the surface (‰)	-6.5	-6.4	-6.5	-6.6	-6.3	-6.5
Isotopic concentration in $H_2{}^{18}O$ of the initial water at –0.35 m (‰)	-6.5	-5.5	-6.4	-6.3	-5.8	-6.4

2 [(a)] Calculated as the water volume divided by the soil volume

3 [(b)] Calculated as the ratio of the soil mass to the soil volume

4

1 Table 3 Dates at which the columns were dismantled. The experiment was launched on April

2 11 2005 at 12h 00 (DoY 101)

Column number	Date of dismantling of the columns	Date of Year (DoY)	Number of days after beginning of drying
6	May 12 2005	132	31
5	June 3 2005	154	53
3	July 11 2005	192	91
2	September 21 2005	264	163
4	December 2 2005	336	235
1	March 15 2006	439 (74+365)	338

3

Table 4 Data used for the estimation of the isotopic composition of the evaporated water vapor and the kinetic fractionation factor. Lines in grey correspond to the same dates but the soil water content and isotopic ratio were sampled over different depths: 0-2.5cm in the top panel and 0-0.5 or 0-0.1cm in the bottom panel.

Decimal Day of the Year	T_{air} (°C)	h_{u_air} (-)	T_{soil} at -2.5cm (°C)	Volumetric water content ($m^3 m^{-3}$)	δ^l_{is} $H_2{}^{18}O$ (°/₀₀)	δ^v_{ia} $H_2{}^{18}O$ (°/₀₀)	Soil surface water pressure (m)	Soil surface relative humidity h_s (-)	Normalized air relative humidity h_a' (-)
Soil water content and isotopic ratio values averaged over 0-2.5 cm									
101.50	24.48	0.77	24.6	0.44	-6.5	-17.0	-0.3	1.000	0.77
132.46	22.02	0.80	22.5	0.34	0.7	-7.4	-2.1	1.000	0.77
138.63	19.95	0.80	20.1	0.33	3.3	-6.2	-2.2	1.000	0.83
145.41	21.46	0.80	21.5	0.31	4.4	-5.3	-2.7	1.000	0.77
154.43	24.87	0.80	24.7	0.26	5.1	-4.1	-4.5	1.000	0.75
164.58	18.61	0.80	19.0	0.26	6.7	-3.5	-4.8	1.000	0.85
171.65	21.00	0.80	21.3	0.20	5.5	-3.9	-9.4	0.999	0.87
181.58	21.25	0.80	21.6	0.15	4.7	-3.3	-20.0	0.999	0.90
192.53	22.75	0.80	22.7	0.13	1.4	-5.4	-34.3	0.998	0.79
203.48	22.15	0.80	22.1	0.11	NA	-5.6	-47.2	0.997	0.79
220.74	22.36	0.60	22.4	0.07	3.1	-9.1	-185.0	0.987	0.60
231.77	22.60	0.60	22.7	0.07	2.3	-9.7	-185.0	0.987	0.59
252.42	21.42	0.50	22.2	0.05	4.6	-9.4	-347.5	0.975	0.47
264.55	20.42	0.50	20.6	0.05	2.8	-10.2	-514.4	0.963	0.50
287.65	22.00	0.40	22.6	0.04	1.9	-10.6	-720.1	0.950	0.39
336.58	22.60	0.20	22.9	0.03	5.6	-12.0	-1929.3	0.871	0.20
439.58	21.97	0.20	22.9	0.02	0.8	-13.1	-4358.3	0.731	0.19
Soil water content and isotopic ratio averaged over 0-0.5 or 0-1 cm									
132.46	22.02	0.80	22.5	0.34	2.1	-7.4	-2.0	1.000	0.77
154.43	24.87	0.80	24.7	0.26	7.4	-4.1	-4.8	1.000	0.75
192.53	22.75	0.80	22.7	0.12	2.9	-5.4	-44.6	0.997	0.79
264.55	20.42	0.50	20.6	0.04	0.5	-10.2	-955.9	0.933	0.50
336.58	22.60	0.20	22.9	0.03	1.5	-12.0	-2156.7	0.857	0.20
439.58	21.97	0.20	22.9	0.02	-0.1	-13.1	-3912.5	0.755	0.19

1 Table 5 Values of the cumulative evaporation (mm) for the six columns estimated by four
2 methods

Method	Column 6	Column 5	Column 3	Column 2	Column 4	Column 1
Method 1: measures of air flow and humidity	35.3	58.4	77.2	105.1	113.3	130.2
Method 2: weighting of the columns	36.8	58.3	79.5	102.6	108.7	133.1
Method 3: trapped volumes	37.2	57.8	80.5	102.9	112.3	132.5
Method 4: soil water storage variation	-	-	-	-	-	120.8

3

4

Table 6 Comparison between the measured isotopic composition of the evaporated water vapor and the use of Eq. (6) with different values of the kinetic fractionation factor:1.014 (turbulent transport), 1.0189 (laminar transport) and 1.0285 (molecular transport). Lines in grey correspond to the same dates but the soil water content and isotopic ratio were sampled over different depths: 0-2.5cm in the top panel and 0-0.5 or 0-0.1cm in the bottom panel.

Day of the Year (DoY)	Measured δ^{v}_{iE} $H_2{}^{18}O$	Calculated δ^{v}_{iE} $H_2{}^{18}O$ with α_K=1.014	Calculated δ^{v}_{iE} $H_2{}^{18}O$ with α_K=1.0189	Calculated δ^{v}_{iE} $H_2{}^{18}O$ with α_K=1.0285
Calculation with soil values averaged over 0-2.5 cm				
101.50	-17.0	-25.1	-29.7	-38.8
132.46	-7.4	-27.1	-31.8	-40.8
138.63	-6.2	-21.1	-25.8	-34.9
145.41	-5.3	-18.4	-23.1	-32.2
154.43	-4.1	-18.8	-23.5	-32.6
164.58	-3.5	-15.5	-20.2	-29.4
171.65	-3.9	-18.7	-23.5	-32.6
181.58	-3.3	-24.5	-29.2	-38.3
192.53	-5.4	-32.5	-37.2	-46.2
220.74	-9.1	-16.1	-20.9	-30.0
231.77	-9.7	-17.1	-21.9	-31.0
252.42	-9.4	-14.6	-19.3	-28.5
264.55	-10.2	-17.1	-21.9	-31.0
287.65	-10.6	-19.3	-24.0	-33.1
336.58	-12.0	-15.4	-20.1	-29.2
439.58	-13.1	-20.8	-25.5	-34.6
Calculation with soil values averaged over 0-0.5 or 0-1 cm				
132.46	-7.4	-21.1	-25.8	-34.9
154.43	-4.1	-6.9	-11.7	-20.9
192.53	-5.4	-25.3	-29.9	-39.0
264.55	-10.2	-21.6	-26.3	-35.4
336.58	-12.0	-20.5	-25.2	-34.3
439.58	-13.1	-22.0	-26.8	-35.8

Table 7 Values of the error retained for the calculation of the error bars on the composition of evaporated water vapor or the derivation of the kinetic fractionation factors. Two cases are considered. Case 1: Analytical and sensor accuracy only. Case 2: Sampling errors

Variable	Analytical and sensor accuracy errors	Sampling errors	Comments on the choice of the values for the sampling errors
Soil and air temperature T_s and T_a	ΔT_s = ΔT_a = 0.2 °C	ΔT_s = ΔT_a =2 °C	Takes into account possible difference between the soil surface and the depth at which the measured is taken for soil temperature and possible heterogeneity above the soil column for air temperature
Air relative humidity h_a	Δh_a = 0.01	Δh_a = 0.1	Takes into account possible heterogeneity of relative humidity above the soil column
Soil water content θ	$\Delta\theta$= 0.01 m^3 m^{-3}	$\Delta\theta$= 0.02 m^3 m^{-3}	Takes into account possible difference in the thickness of the soil used to estimate the soil surface water content and inaccuracy in the estimation of the retention curve
Water vapor isotopic composition δ^v_{iout}	$\Delta\delta^v_{O18out}$ = 0.5	$\Delta\delta^v_{O18out}$ = 1.25	Estimation based on differences between the values of different columns (see Fig. 9)
Soil surface liquid isotopic composition δ^l_{is}	$\Delta\delta^l_{O18s}$ = 0.5	$\Delta\delta^l_{O18s}$ = 5	Estimation based on differences between values averaged over the 0-2.5 cm or 0-0.5 or 0-1 cm depths (see Table 4)
Kinetic fractionation factor α_K	$\Delta\alpha_{KO18}$= 0.0096	$\Delta\alpha_{KO18}$= 0.0096	No difference

Table 8 Estimation of the isotopic composition of the liquid water required to match the measured value of the isotopic composition of the evaporated water vapor with the calculated value using Eq. (6). Standard errors calculated using the formulae of Appendix D are also given when sampling errors are taken into account. Lines in grey correspond to the same dates but the soil water content and isotopic ratio were sampled over different depths: 0-2.5cm in the top panel and 0-0.5 or 0-0.1cm in the bottom panel.

		Calculation with α_K = 1.014			**Calculation with α_K = 1.0189**			**Calculation with α_K = 1.0285**		
Decimal Day of the Year (DoY)	Measured at the surface (Maximum in the profile)	Calculated average	Standard error without α_K	Standard error with α_K	Calculated average	Standard error without α_K	Standard error with α_K	Calculated average	Standard error without α_K	Standard error with α_K
Soil values are averaged over the 0-2.5 cm depth										
101.5	-6.5	-4.5	2.5	3.3	-3.4	3.8	4.4	-1.1	4.5	5.1
132.46	0.7	5.3	2.5	3.3	6.3	3.9	4.5	8.5	4.6	5.1
138.63	3.3	6.4	2.6	3.3	7.4	4.0	4.4	9.4	4.8	5.2
145.41	4.4	7.2	2.6	3.2	8.1	4.0	4.4	10.1	4.8	5.2
154.43	5.1	8.0	2.6	3.2	8.9	4.0	4.4	10.8	4.8	5.1
164.58	6.7	9.5	2.6	3.3	10.5	3.9	4.5	12.6	4.7	5.2
171.65	5.5	8.8	2.5	3.3	9.8	3.9	4.4	11.9	4.7	5.2
181.58	4.7	9.4	2.5	3.3	10.4	3.9	4.4	12.5	4.7	5.2
192.53	1.4	6.9	2.6	3.2	7.9	4.0	4.4	9.8	4.8	5.1
220.74	3.1	6.0	2.3	4.4	7.8	3.6	5.3	9.6	4.8	5.2
231.77	2.3	5.4	2.3	4.4	7.3	3.6	5.3	11.6	4.1	5.6
252.42	4.6	7.3	2.1	5.3	9.8	3.5	6.0	11.1	4.1	5.6
264.55	2.8	6.3	2.2	5.2	8.6	3.6	5.9	14.7	3.8	6.2
287.65	1.9	7.2	2.1	6.1	10.1	3.4	6.6	13.3	4.0	6.1
336.58	5.6	8.4	2.2	7.7	12.0	3.5	8.2	15.8	3.7	6.8
439.58	0.8	6.7	3.7	8.0	10.2	5.3	8.9	19.5	3.9	8.4
Soil values are averaged over the 0-0.5 or 0-1 cm depth										
132.46	2.1 (2.1)	5.3	2.5	3.3	6.3	3.9	4.4	17.3	7.2	10.1
154.43	7.4 (7.4)	8.0	2.6	3.2	8.9	4.0	4.4	8.5	4.6	5.1
192.53	2.9 (2.9)	6.9	2.6	3.2	7.8	4.0	4.4	10.8	4.8	5.1
264.55	0.5 (5.1)	6.1	2.4	5.1	8.3	3.7	5.8	9.7	4.8	5.1
336.58	1.5 (11.6)	8.3	2.3	7.7	12.0	3.6	8.2	12.8	4.3	6.2
439.58	-0.1 (11.5)	6.9	3.3	7.9	10.4	4.8	8.6	19.4	4.0	8.4

Table 9 Estimation of the kinetic fractionation factor for $H_2{}^{18}0$ by using Eq. (16). Calculated values of the standard error as well as their minimum and maximum are also reported, based on estimates of sampling errors (Appendix E). Values are given in per mil $(1-\alpha_K)$ *1000 and $\sigma_{\alpha K}$*1000. Lines in grey correspond to the same dates but the soil water content and isotopic ratio were sampled over different depths: 0-2.5cm in the top panel and 0-0.5 or 0-0.1cm in the bottom panel. For the last three lines figures in parenthesis provide the results when the soil water content and liquid isotopic ratio were taken at the peak.

Decimal Day of the Year	Averaged $\alpha_K{}^{18}O$	Minimum $\alpha_K{}^{18}O$	Maximum $\alpha_K{}^{18}O$	Standard error $\alpha_K{}^{18}O$
Soil values are averaged over the 0-2.5 cm depth				
101.50	5.4	-14.3	25.0	10.7
132.46	-6.3	-29.3	16.8	11.7
138.63	-1.1	-19.2	17.0	11.5
145.41	0.4	-16.8	17.6	11.8
154.43	-0.8	-19.5	17.9	12.2
164.58	1.6	-14.7	17.9	10.8
171.65	-1.1	-18.4	16.2	11.0
181.58	-7.6	-33.4	18.3	12.6
192.53	-13.7	-50.6	23.3	16.8
220.74	6.8	-5.3	19.0	6.4
231.77	6.4	-5.4	18.1	6.3
252.42	8.8	-1.1	18.7	5.1
264.55	6.9	-3.0	16.8	5.2
287.65	5.1	-2.0	12.3	4.1
336.58	10.6	3.5	17.6	3.5
439.58	6.1	-1.4	13.6	3.8
Soil values are averaged over the 0-0.5 or 0-1 cm depth				
132.46	0.0	-15.4	15.3	10.6
154.43	11.0	-20.9	42.9	15.0
192.53	-6.1	-32.3	20.1	13.2
264.55	2.3 (11.5)	-5.9 (-0.1)	10.4 (23.0)	5.1 (5.6)
336.58	5.3 (17.8)	-0.4 (10.4)	11.0 (25.2)	3.2 (3.8)
439.58	4.8 (18.9)	-1.7 (11.6)	11.3 (26.3)	3.5 (3.8)

1 Fig.1. Photo of the experimental set up.

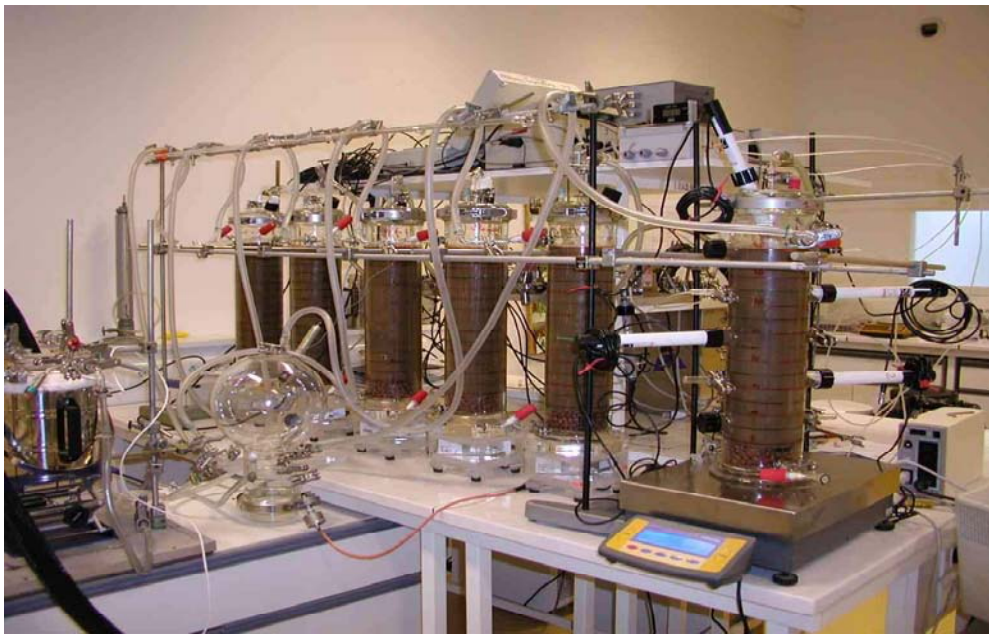

2

3 Fig. 2. Scheme of the experimental set up (view from the top).

4

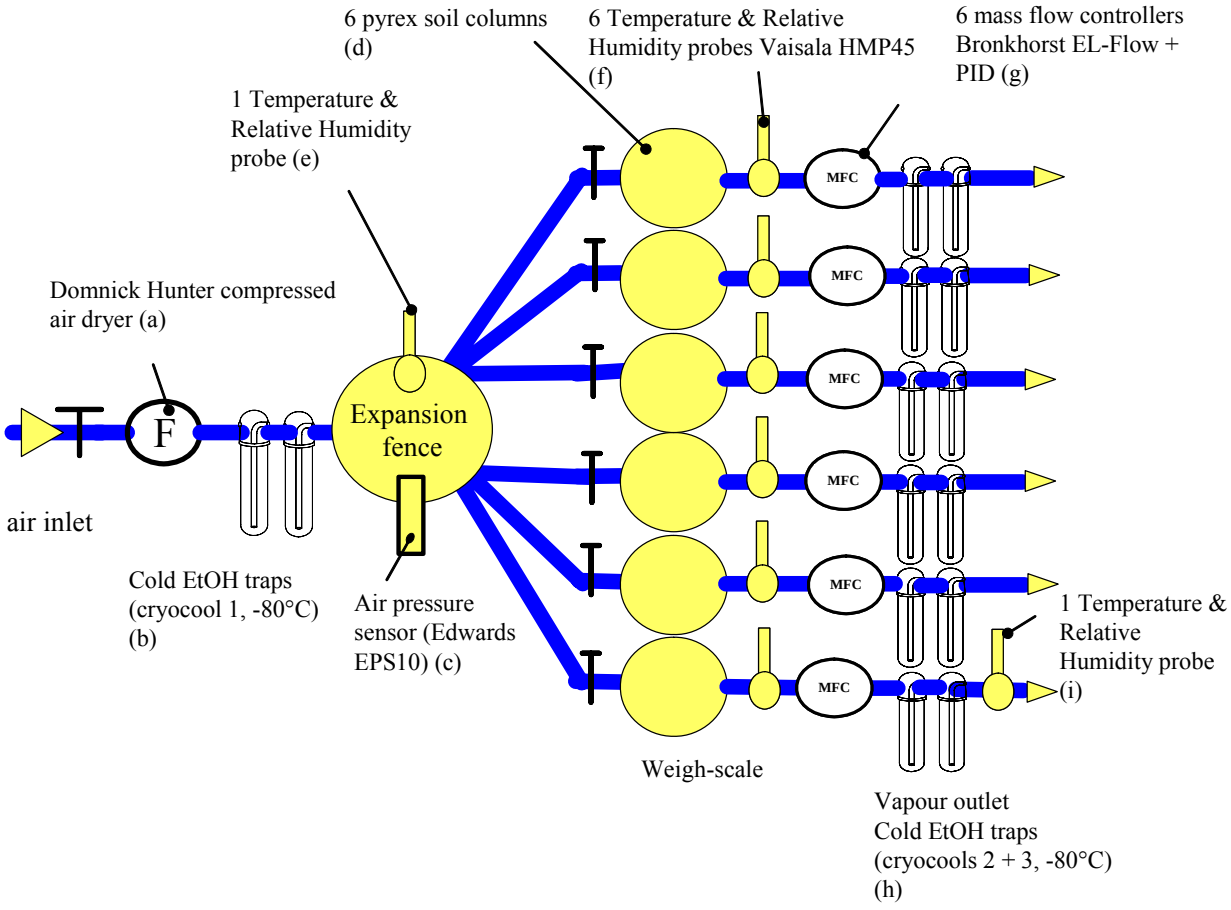

1 Fig. 3: Time evolution of air temperture and relative humidity at the outlet of column 1

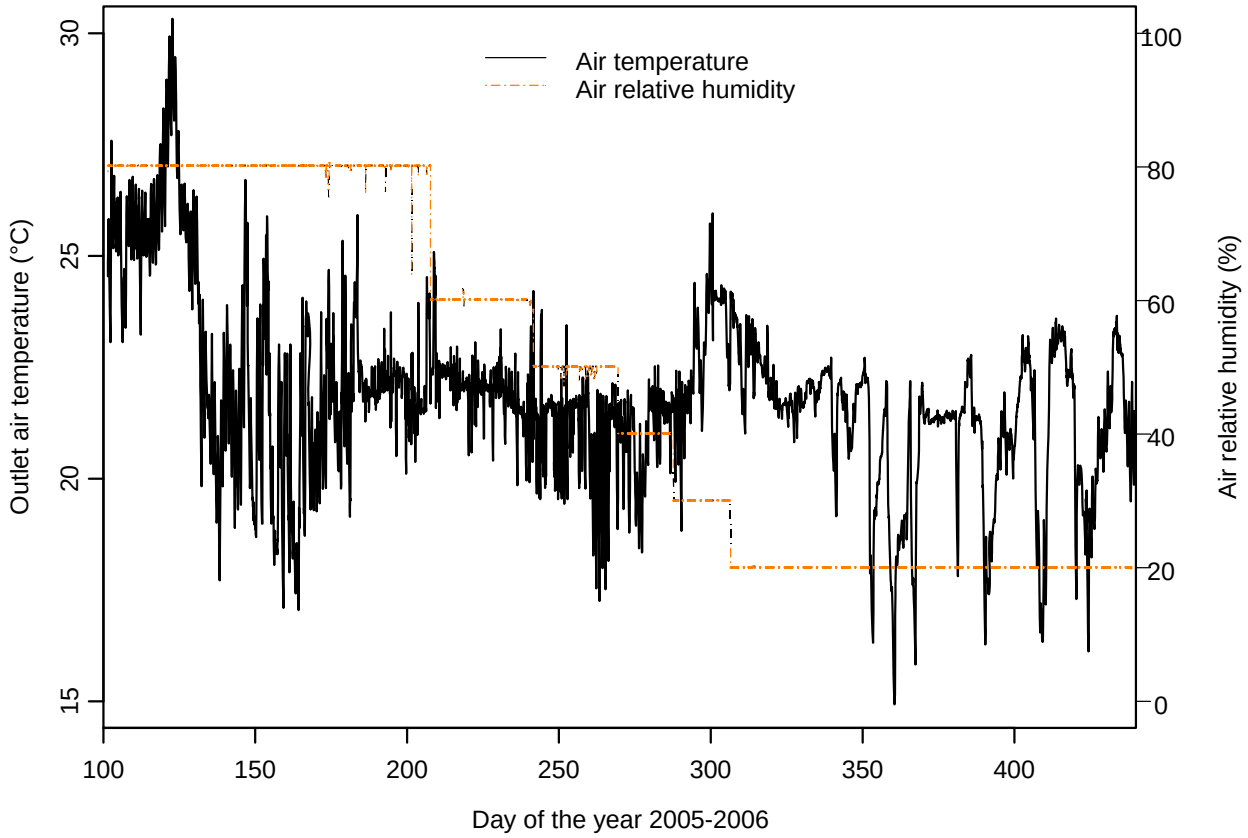

2

Figure 4. Evolution of the oxygen 18 composition of the liquid water as function of the gravimetric water content (kg kg^{-1}). The results were obtained after 15h of distillation and corrected for the efficiency of the extraction. The target initial oxygen 18 isotopic composition of the liquid water is -7.10 ± 0.05 ‰. Vertical bars correspond to the analytical errors (± 0.1 ‰).

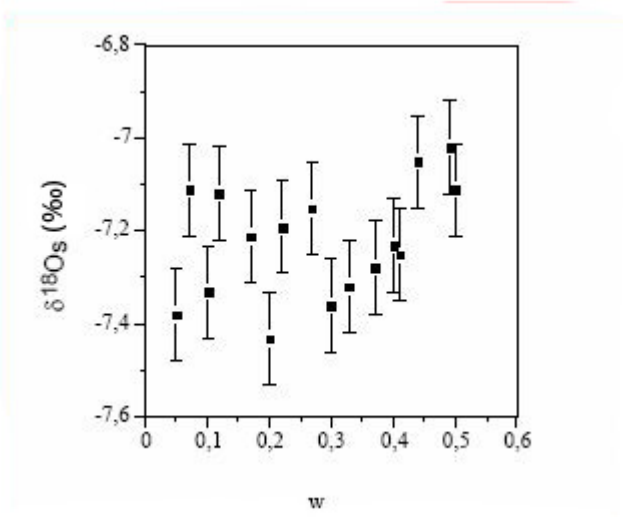

Figure 5. Retention curve $h(\theta)$ of the soil. The squares correspond to the measured (h,θ) couples at –2.5 cm (full square), -8 cm (crosses), -16 cm (open triangles). The continuous line corresponds to the fitted Van Genuchten model $\frac{\theta}{\theta_{sat}} = \left(1+\left(\frac{h}{h_{VG}}\right)^{n}\right)^{-m}$ *with* $m = 1-\frac{2}{n}$ for the -2.5 cm data. Values of the parameters are n=2.36, h_{VG}=-1.05 m, θ_{sat}=0.444.

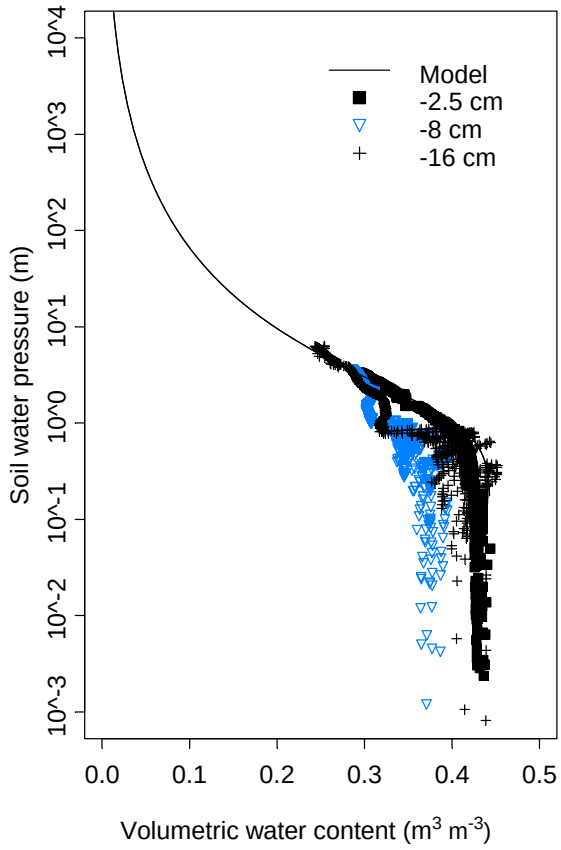

Figure 6. Comparison of the cumulative evaporation (left) and the instantaneous flux (right) estimated by using the measures of air flow and water vapor humidity at the outlet (full black), the weighting of the columns (dashed black), the trapped water volume at the outlet (dashed light) and the calculated soil water storage (full light) for column 1 (top) and column 4 (bottom).

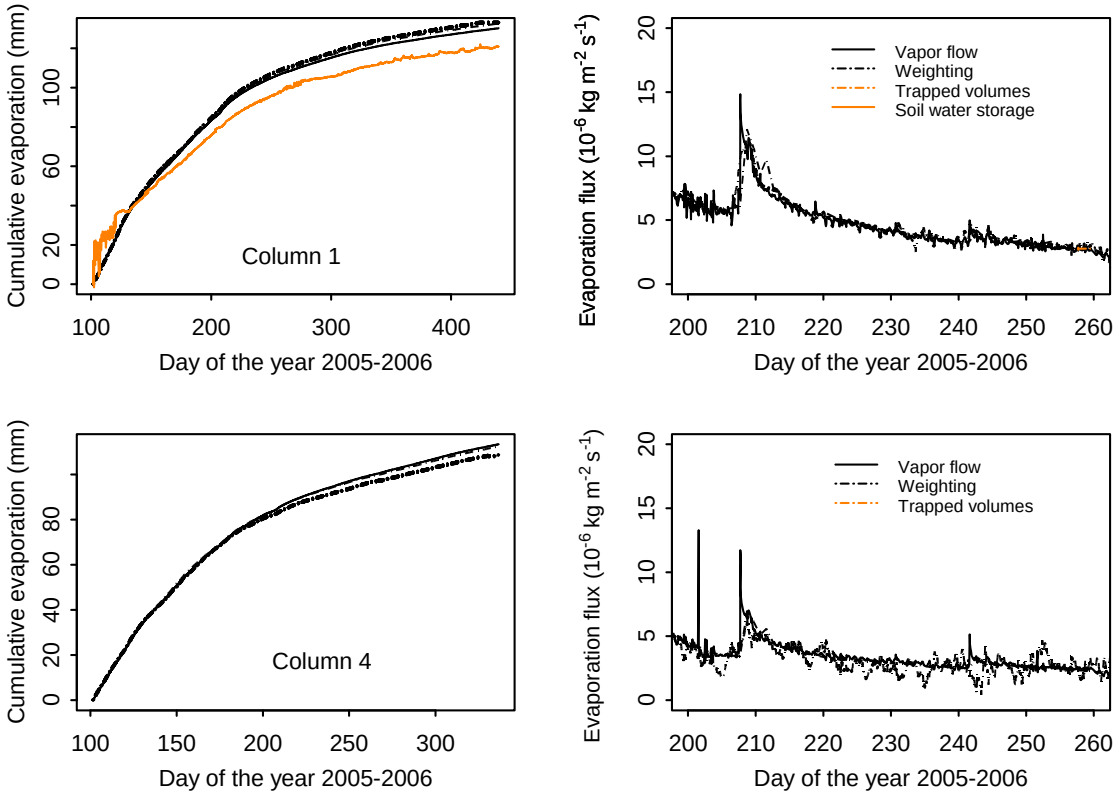

Figure 7. Evaporation flux (top) and cumulative evaporation (bottom) of the six columns. Values were calculated using Method 1.

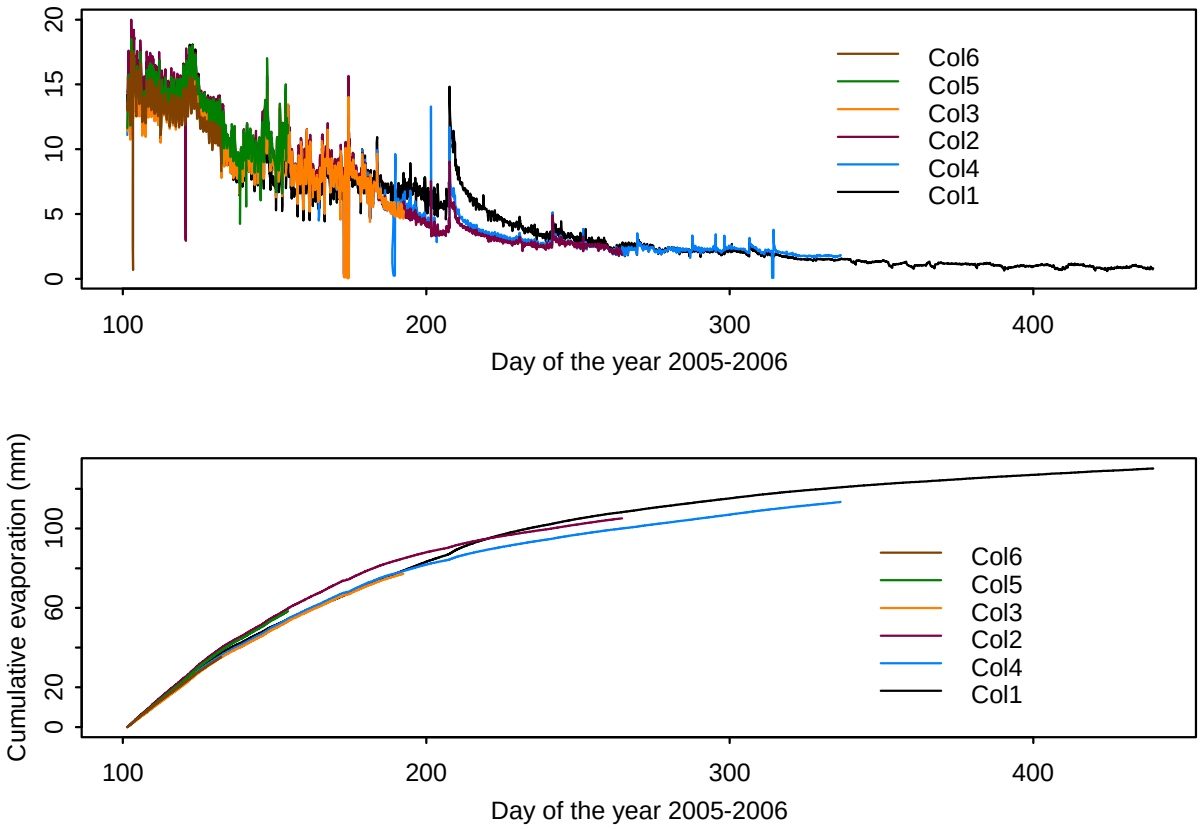

Figure 8. Volumetric water content (left) and oxygen 18 isotopic ratio (right) (in °/∞) of the six soil columns when they were dismantled. The vertical straight lines are the initial values. DoY is Day of the Year

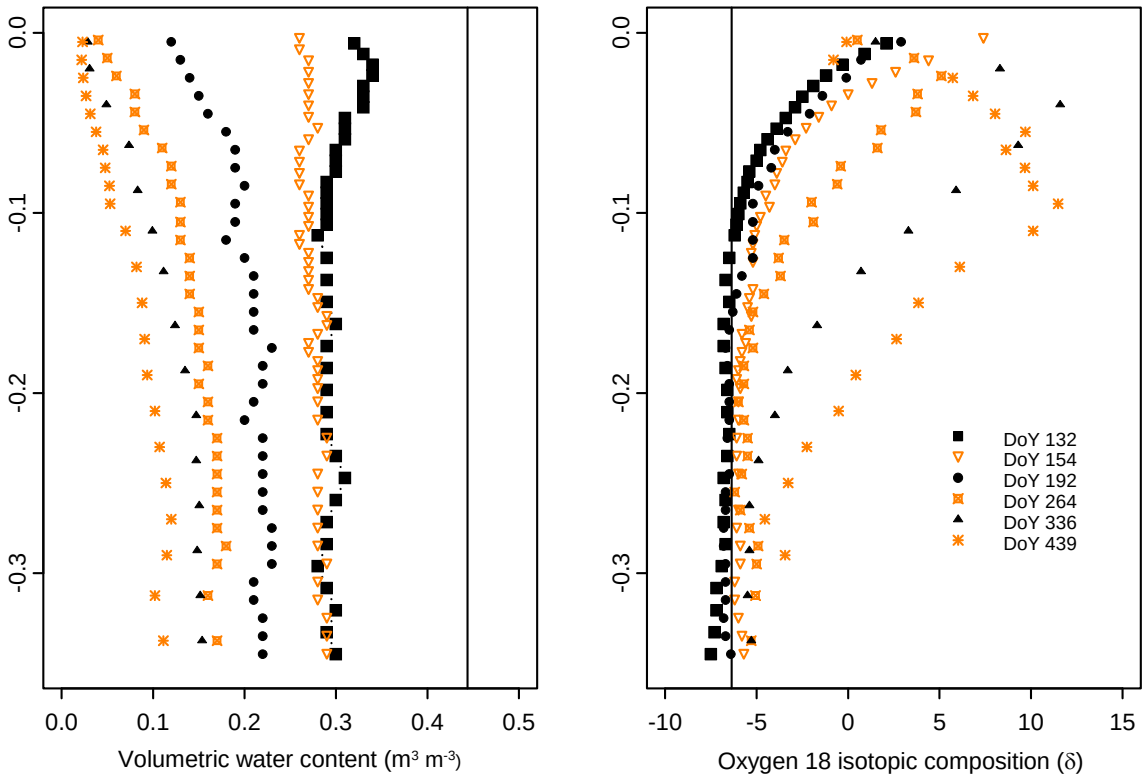

Figure 9. Time evolution of the oxygen 18 isotopic ratio of the evaporated water vapor for the six columns. The horizontal black line gives the composition of the initial water –6.4 °/∞. The sampling frequency is twice a day from DoY 101 to 136; once a day from DoY 137 to 224 and then about one sample every two or three days.

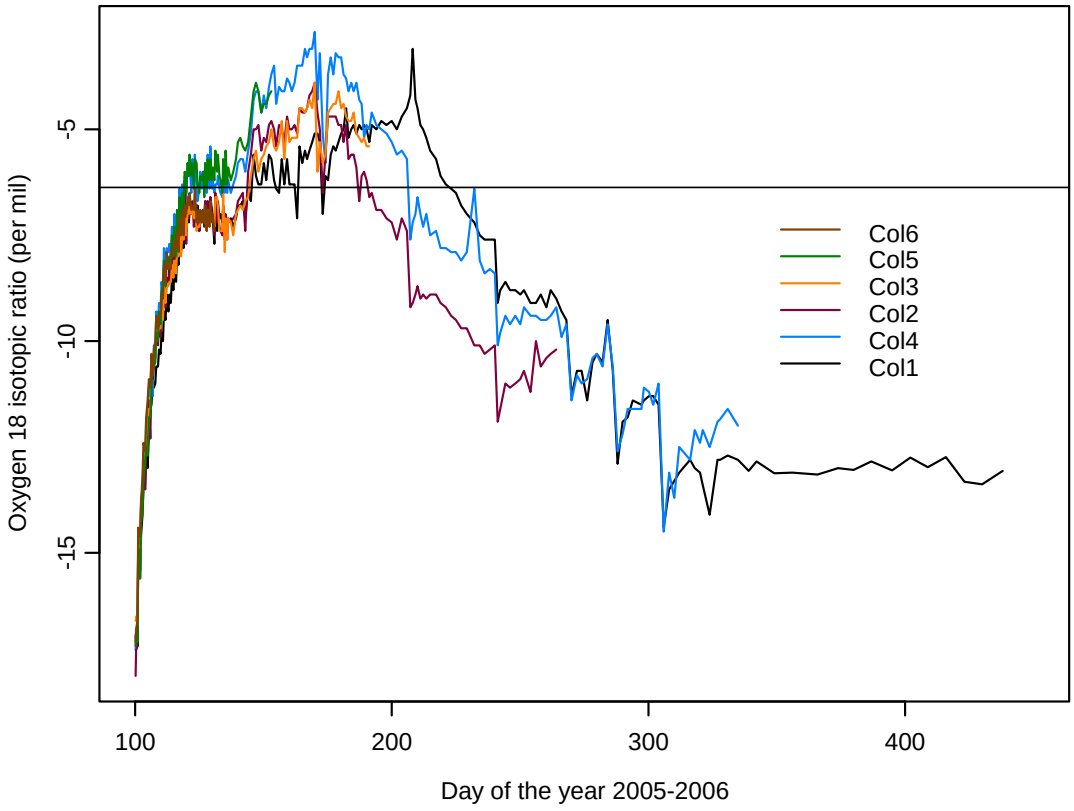

Figure 10. Comparison of the measured oxygen 18 isotopic composition of the evaporated water vapor (squares) and the calculated one using Eq. (6) with α_K=1.0189 (points). Values of the standard error, as well as their minimum and maximum, estimated using analytical and sensor accuracy errors are also plotted. Results with soil water content and liquid isotopic ratios sampled over the 0-2.5 cm and 0-0.5 or 0-1 cm layers are represented in the top and bottom panels, respectively.

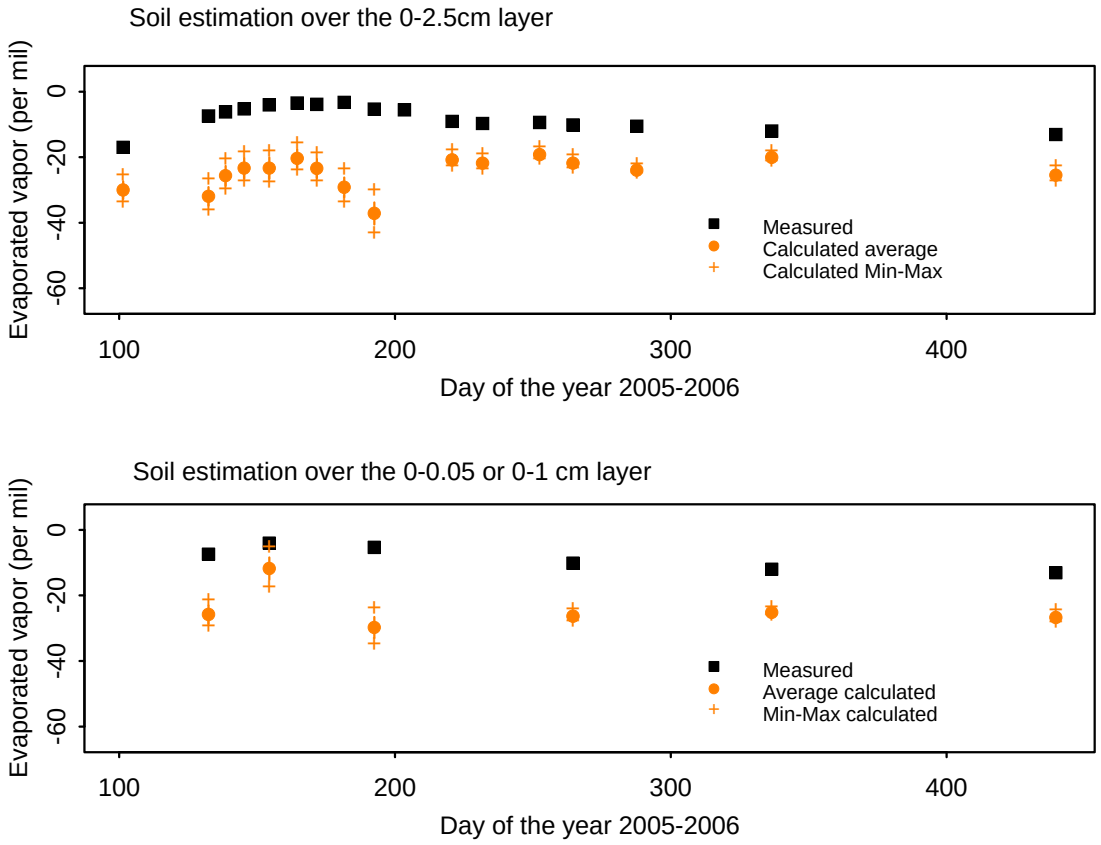

Figure 11. Comparison of the measured oxygen 18 isotopic composition of the evaporated water vapor (squares) and the calculated one using Eq. (6) with α_K=1.0189 (points). Values of the standard error, as well as their minimum and maximum, estimated using sampling errors are plotted. Results with soil water content and liquid isotopic ratios sampled over the 0-2.5 cm and 0-0.5 or 0-1 cm layers are represented in the top and bottom panels, respectively.

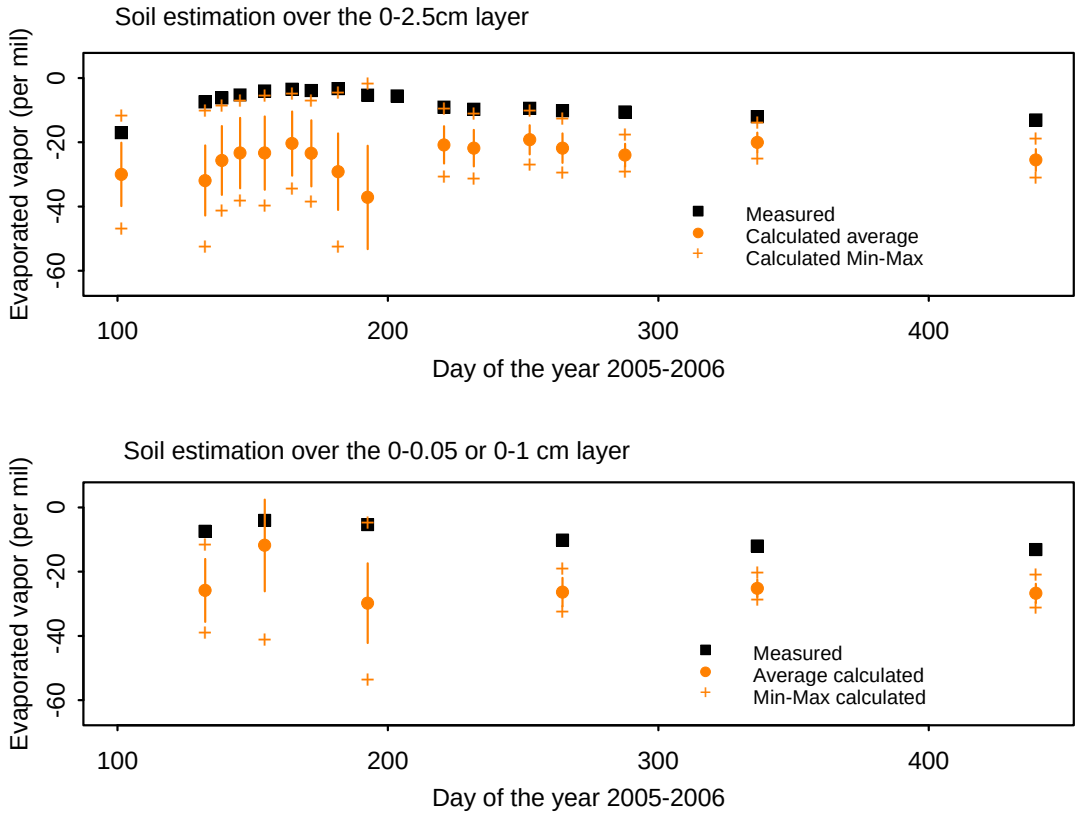

Figure 12. Contribution of the various sources of errors on the calculated isotopic composition of the evaporated water vapor for oxygen 18 for the sampling errors and α_K=1.0189. Top panel: when error on α_K is not taken into account. Bottom panel: when error on α_K is taken into account. The dates in abscissa correspond to the lines in Table 6 in the same order. In the legend the labels refer to errors on soil temperature T_s (Ts), isotopic composition of the soil surface liquid water δ_{is}^{l} (deltal), water vapor above the soil column δ_{ia}^{v} (deltair), air temperature T_a (Ta), air relative humidity h_a (ha), soil water content θ (theta) and kinetic fractionation factor α_K (alphak).

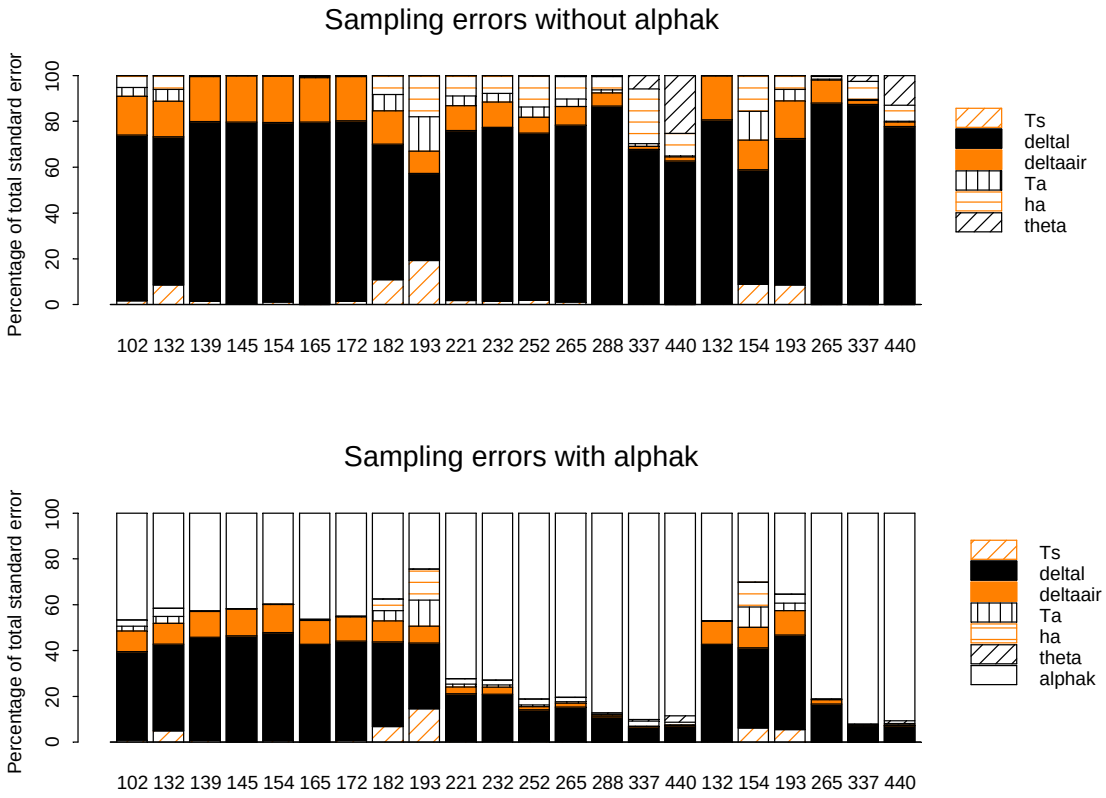

Figure 13. Value of the isotopic composition of the soil liquid water, required so that the isotopic composition of the evaporated water vapor calculated using Eq. (6) matches the measured value. The standard error, minimum and maximum values estimated using sampling errors are also plotted. Measured values correspond to the 0-2.5 cm depth layer.

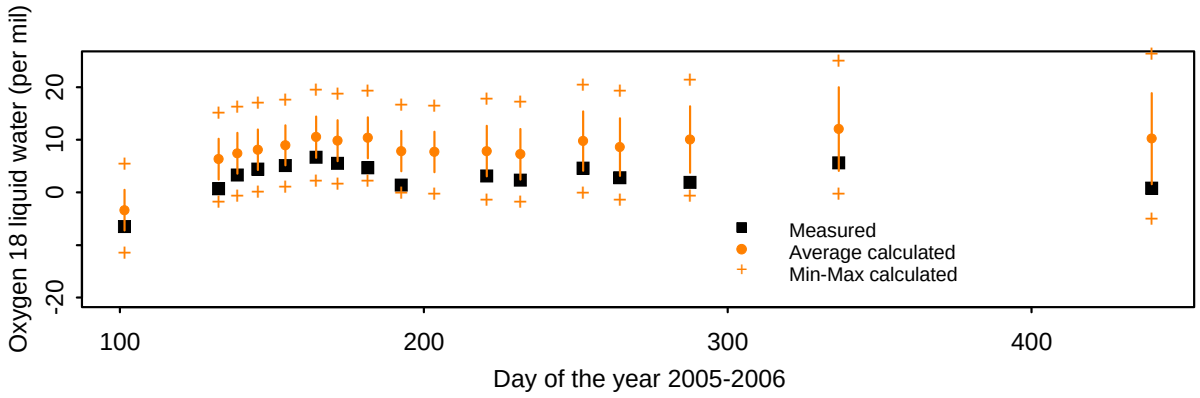

Figure 14 Contribution of the various sources of errors on the calculated isotopic composition of the soil liquid water required so that the isotopic composition of the evaporated water vapor calculated using Eq. (6) matches the measured value calculated using oxygen 18 and the sampling errors. Top: error on the kinetic fractionation factor is not considered. Bottom: Error on the kinetic fractionation factor is considered. The dates in abscissa correspond to the lines in Table 8 in the same order. In the legend the labels refer to errors on soil temperature T_s (Ts), water vapor above the soil column δ_{ia}^{v} (deltair), air temperature T_a (Ta), air relative humidity h_a (ha), soil water content θ (theta) and kinetic fractionation factor α_K (alphak).

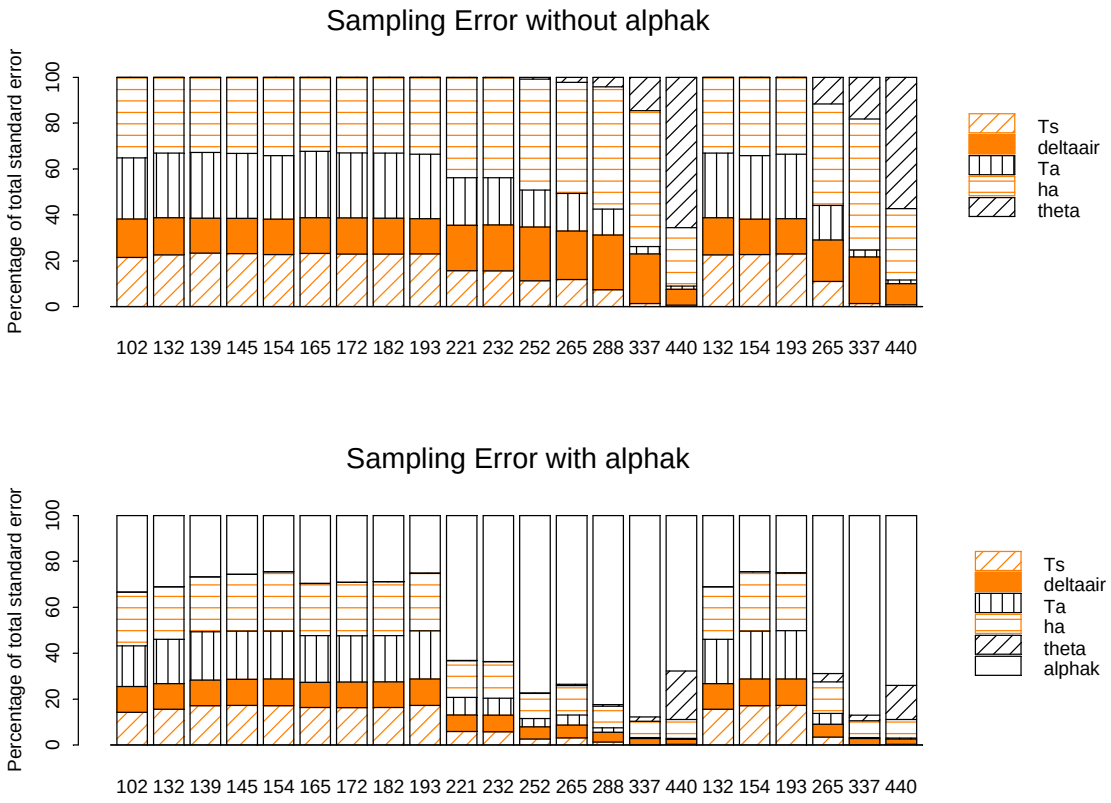

Figure 15. Contribution of the various sources of errors on the calculated kinetic fractionation factor for oxygen 18 and for the sampling errors. The dates in abscissa correspond to the lines in Table 9 in the same order. In the legend the labels refer to errors on soil temperature T_s (Ts), isotopic composition of the soil surface liquid water δ_{is}^{l} (deltal), water vapor above the soil column δ_{ia}^{v} (deltair), air temperature T_a (Ta), air relative humidity h_a (ha), soil water content θ (theta).